1-1-2008

Fault detection of fault ride through for doubly-fed induction generator based wind energy systems

Shoba AD Ramroop
Ryerson University

Fault Detection of Fault Ride Through for Doubly-Fed Induction Generator based Wind Energy Systems

by

SHOBA A.D. RAMROOP
B.Eng, Ryerson University, 2003

A project
presented to Ryerson University
in partial fulfillment of the
requirements for the degree of
Masters in Engineering
in the Program of
Electrical and Computer Engineering

Toronto, Canada

I hereby declare that I am the sole author of this project. I authorize Ryerson University to lend this project to other institutions or individuals for the purpose of scholarly research.

I further authorize Ryerson University to reproduce this project by photocopying or by other means, in total or in part, at the request of other institutions or individuals for the purpose of scholarly research.

Fault Detection of Fault Ride Through for Doubly-Fed Induction Generator based Wind Energy Systems

by

SHOBA A.D. RAMROOP
B.Eng, Ryerson University, 2003

ABSTRACT

Fault detection and mitigation is of high importance for existing DFIG based wind energy conversion systems. Keeping the doubly-fed induction generator (DFIG) online during faults is desirable since reconnection can cause system instability. Grid disturbances induce large rotor currents at the machine side power electronic converter. The currents exceed the device ratings potentially causing damage. A stand alone active crowbar protection system is proposed in this project where the active crowbar is connected to the rotor windings providing a bypass path for the excessive current to dissipate across. The fault detection algorithm are developed using negative sequence detection method, which detected the negative sequence instantaneous power. The protection system disconnects the converter from the system while activating crowbar for providing fault current circulation. The overall wind energy system with active crowbar was modelling in Matlab/Simulink and simulation results verify the functionality of the proposed protection system.

ACKNOWLEDGEMENTS

I wish to express my deep gratitude to my supervisor, Professor Dewei Xu for his support and the knowledge he shared during my graduate studies at Ryerson University.

I would like to thank Honeywell for their support and my fellow colleagues for sharing their power electronic expertise.

I would also like to thank my fellow peers, Kostya and Ehsan for their invaluable help.

With great pleasure I share my achievement with my family. To my parents, Arnold and Chu whose presence, constant support, encouragement and understanding made this work possible. To my brother, Andrew, whose constant motivation was inspiring.

TO MY GRANDFATHER

TABLE OF CONTENTS

CHAPTER 1 INTRODUCTION 1

1.1 Background 1

1.2 Wind Energy Conversion Systems 3

1.2.1 Fixed Speed WECS 4

1.2.2 Variable Speed WECS 5

1.2.3 Doubly-Fed Induction Generator 6

1.3 Low Voltage Ride Through (LVRT) & Grid Connection Code 8

1.4 Motivation 11

1.5 Report Organization 13

CHAPTER 2 DFIG ANALYSIS 14

2.1 System Configuration 14

2.1.1 AC/DC/AC Converter Topology 15

2.2 DFIG Model and Control 16

2.2.1 DFIG Equivalent Mathematical Model 16

2.2.2 Machine Side Converter Control 18

2.2.3 Grid Side Converter Control 23

2.3 Turbine Operation 24

2.4 DFIG Normal Operation Analysis 26

2.5 Summary 31

CHAPTER 3 ANALYSIS OF DFIG DURING FAULT 32

3.1 Introduction 32

3.2 DFIG during Fault 33

3.2.1 Three Phase Shorted to Ground 33

3.2.2 Single Phase Shorted to Ground 36

3.2.3 Two Phase Shorted 38

3.3 Summary 40

CHAPTER 4 FAULT DETECTION 42

4.1 Fault Introduction 42

4.2 Active Crowbar 43

4.3 Fault Detection Methods 44

4.3.1 Fault Detection using Rotor Current 45
4.3.2 Fault Detection using Voltage RMS Value of Stator Voltage 46
4.3.3 Fault Detection using Instantaneous Pseudo-Power Detection 48
4.4 DFIG with Fault Detection System 51
4.4.1 Three Phase Shorted to Ground 52
4.4.2 Single Phase Shorted to Ground 55
4.4.3 Two Phase Shorted 57
4.5 Summary 59
CHAPTER 5 CONCLUSIONS 60
5.1 Conclusions 60
5.2 Major Contribution 61
5.3 Future Work 61
REFERENCES 62
APPENDIX A 66
APPENDIX B 67
APPENDIX C 68

LIST OF FIGURES

Figure 1-1 WWEC Total Installed Capacity Prediction, 2006 2
Figure 1-2 Wind Turbine Installation for 2006 [3] 2
Figure 1-3 Performance Coefficient, Cp vs. TSR [4] 4
Figure 1-4 Fixed Speed Squirrel Cage Induction Generator 4
Figure 1-5 Variable Speed Induction Generators 5
Figure 1-6 Synchronous Generator 6
Figure 1-7 Wind Turbine System 7
Figure 1-8 Back-to-back Converter 7
Figure 1-9 DFIG Power Flow Diagram 8
Figure 1-10 Typical LVRT Characteristic 9
Figure 1-11 DFIG with Active Crowbar 12
Figure 2-1 DFIG System Configuration 15
Figure 2-2 AC/DC/AC Converter 16
Figure 2-3 DFIG Equivalent Circuit 17
Figure 2-4 Vector Diagram of Stator Flux FOC 19
Figure 2-5 Machine Side Converter Control Block 22
Figure 2-6 Grid Side Converter 23
Figure 2-7 Grid Side Converter Control Block 24
Figure 2-8 MPPT Characteristic 25
Figure 2-9 WECS Block Diagram 26
Figure 2-10 DFIG System Performance Characteristic 29
Figure 2-11 Rotor Reference Current and Stator Flux Magnitude 30
Figure 2-12 DFIG Rotor Current 31
Figure 3-1 DFIG Characteristics under 3ϕ Fault 34
Figure 3-2 Rotor Voltage 35
Figure 3-3 Rotor Current under 3ϕ Fault Condition 36
Figure 3-4 DFIG Characteristics under Single Phase Short Condition 37
Figure 3-5 Rotor Current under Single Phase Short Condition 38

Figure 3-6 DFIG Characteristic under Two Phase Fault Condition 39
Figure 3-7 Rotor Current under Two Phase Fault Condition 40
Figure 4-1 Active Crowbar – Rectifier Configuration 43
Figure 4-2 Active Crowbar – Thyristor Configuration 44
Figure 4-3 DFIG with Active Crowbar Protection System 45
Figure 4-4 Mean Value Theorem Control Block 47
Figure 4-5 Rotor Current Response with Crowbar Activated, ... 48
Figure 4-6 Instantaneous Pseudo-Power Detection Control Block 49
Figure 4-7 Positive and Negative Pseudo-Power during 1Φ Ground Fault 51
Figure 4-8 Rotor Current during 3Φ Fault using Sp Detection 53
Figure 4-9 Rotor Current under Instantaneous Stator Voltage Control 54
Figure 4-10 DFIG Characteristic with Active Crowbar under 3ϕ Short 55
Figure 4-11 Rotor Current under Single Phase Fault with Active Crowbar 56
Figure 4-12 DFIG Characteristic with Active Crowbar under Single Phase Fault 57
Figure 4-13 Apparent Power Terms under Two Phase Fault Condition 58
Figure 4-14 Rotor Current under Two Phase Fault Condition with Active Crowbar 59

LIST OF TABLES

Table 1-1 Summary of LVRT Alternatives [9] 10
Table 2-1 DFIG Model Parameters 27
Table 2-2 PI Controller Gain Terms 29

List of symbols

General Variables

Φ	phase
p	poles

Turbine Variables

T_{mech}	mechanical torque
P_{mech}	mechanical power
P_{wind}	wind power
λ	tip speed
ρ	air density
C_p	performance Coefficient

DFIG Variables

v_{dqs}	stator voltage
v_{dqr}	rotor voltage
v_{dqs}	stator current
i_{dqr}	rotor current
s	slip
ω_s	stator frequency
ω_r	rotor frequency
ω_e	synchronous reference frame frequency
R_s	stator resistance
R_r	rotor resistance
L_s	stator side leakage inductance
L_r	rotor side leakage inductance
P_s	stator power
P_r	rotor power
F	friction coefficient
H	inertia
T_e	electrical torque

DFIG Control Parameters

K_i	integral gain term
K_p	proportional gain term

Active Crowbar Control Parameters

K	overload constant
S_p	positive apparent power
S_n	negative apparent power
v_{dq}^{p}	positive sequence voltage
v_{dq}^{n}	negative sequence voltage
u_{dq}^{p}	positive reference voltage
u_{dq}^{n}	negative reference voltage

CHAPTER 1 INTRODUCTION

1.1 Background

Wind energy has become a popular alternative power source, which can be seen in the significant reduction of greenhouse gas emissions from traditional fossil energy. Compared with other alternative energy sources available, such as solar and hydro-electric, wind offers lowest cost per kilo-watt hour. With technology advancement, the current systems require less maintenance and the operating life is far extended. Wind energy systems have attracted tremendous investment in the wind energy system, featuring fast growth in the last few years.

Many European countries have opted installing large scale turbines and wind farms in conjunction with traditional fuel generating systems in hopes of reducing and/or eliminating fossil fuels. As of 2006, it was reported Europe accounts for approximately 65% of the world's total installed capacity [1], approximately 74,000MW with 19% growth over the last year, producing an estimated 100TWh of electricity. In North America, 22% of the world's new wind capacity was installed in the US and Canada, where the annual market increased by a third in 2005. Hydro-Quebec has established multiple wind farms along the Gaspe Peninsula in Eastern Quebec along the St. Lawrence River capable of producing 35,000 MW [2]. The wind turbine stationed at the Ontario Power Generation facility in Pickering, Ontario generates approximately 2,900 MW/hours capable of supplying electricity to 330 homes. Under full capacity the turbine is capable of producing enough electricity to power 1800 homes. Canada exceeded initial estimates with installed capacity doubling from 683 MW in 2005 to 1459 MW at the end of 2006. The Canadian Wind Energy Association (CanWEA) expects the wind energy industry in Canada to boom as provincial governments are now targeting to have a minimum of 10,000 MW of installed wind energy capacity in place by 2015 [1].

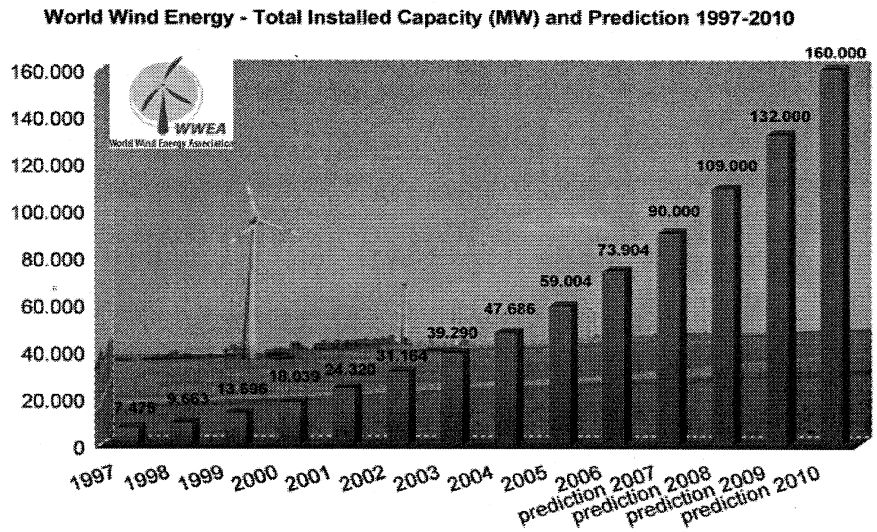

Figure 1-1 WWEC Total Installed Capacity Prediction, 2006

From Figure 1-1, the World Wind Energy Council (WWEC) predicts the total installed capacity will top 160,000MW by 2010. Currently, wind power accounts for 1% of the world's total electricity generation, paving the way is Germany whose total wind power accounts for 7.3% and is expected to increase to 12.3% sooner then the expected target date of 2010. As Germany and Denmark provide the standard for sustainable energy solutions, many other countries are following as the benefits are inherently visible from an ecological standpoint. Based on this trend, wind farms are increasing the capacity by installing larger turbines to meet demands, inadvertently the need to address grid connection codes, fault diagnosis and mitigation, and adherence to power quality requirements becomes of importance.

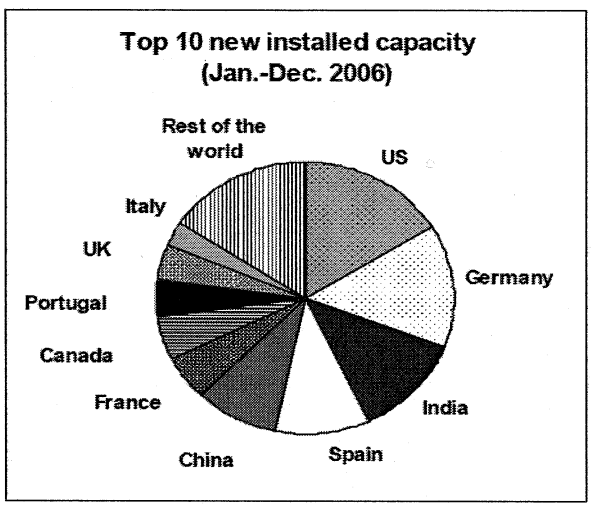

New capacity	MW	Market share
US	2,454	16.1%
Germany	2,233	14.7%
India	1,840	12.1%
Spain	1,587	10.4%
China	1,347	8.9%
France	810	5.3%
Canada	776	5.1%
Portugal	694	4.6%
UK	634	4.2%
Italy	417	2.7%
Top 10 – Total	**12,792**	**84.2%**
Rest of the world	**2,405**	**15.8%**
World total	**15,197**	

Figure 1-2 Wind Turbine Installation for 2006 [3]

1.2 Wind Energy Conversion Systems

The premise of wind energy conversion systems (WECS) is the ability of extracting energy from the wind and converting it into useful electrical power. Mechanical energy is generated when the wind flows through the turbine's propeller blades causing the shaft torque. Because the generator is coupled to the turbine, electricity is generated from mechanical power.

The power extracted from the wind, P_{wind}, can be represented by the following equation,

$$P_{wind} = \frac{\rho}{2} C_p(\lambda,\theta) A_R v_w^3 \tag{1.1}$$

The performance characteristic of the turbine's propeller, C_p, which is usually represented by the turbine tip speed ratio, λ and the pitch angle, θ, is a function of the wind speed, rotational speed of the turbine and the turbine blade parameters. The curves in Figure 1-3, illustrates how the performance coefficient, C_p is a function of the tip-speed ratio (TSR) under three different pitch angles. With different pitch angle, P_{wind} will be at the maximum when TSR is optimized.

The method of controlling the turbine strongly affects the power generation of the system [4]; hence the common control scheme used is variable speed control. The most economical condition for power generation is during low to medium wind speeds, where the system operates at maximum C_p. The rotor speed is adjusted to capture maximum wind energy at optimized TSR. During high wind speed conditions, the input power to the turbine is limited by the pitch control, the pitch angle is increased or decreased in order to shed some of the aerodynamic power developed across the propeller blades, and this reduces the excessive mechanical stress imposed on the gear-box and generator shaft. Because turbines typically operate between 6.0 m/s to 8.0 m/s with the maximum wind speed around 14m/s. Beyond that, the turbine's operation is prohibited in order to protect the whole system.

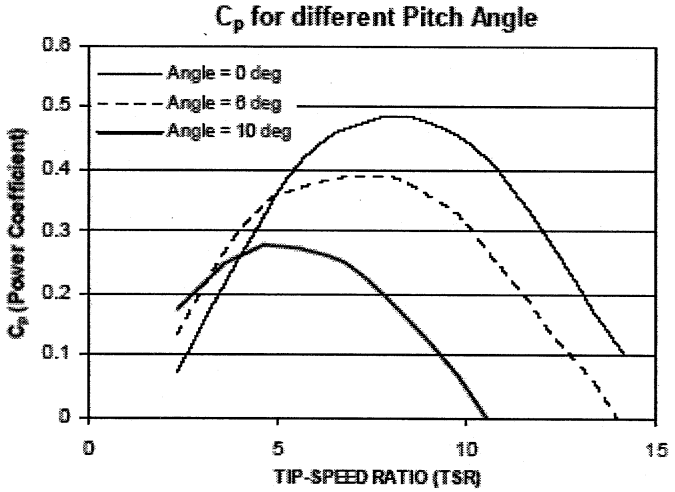

Figure 1-3 Performance Coefficient, Cp vs. TSR [4]

Wind turbine systems can operate in either a fixed-speed or variable-speed conditions depending on the generating system used. The next few sections compare the two types of generators and discuss the characteristic features of each topology. This will lead into the introduction of the doubly-fed induction generator (DFIG), which are dominant in the current wind industry.

1.2.1 Fixed Speed WECS

As shown in Figure 1-4, a fixed-speed wind turbine system composes of a gear-coupled induction generator, which is directly connected to the utility grid. Reactive power compensation is achieved by adding compensating capacitors to the stator windings, providing excitation current for generator stators. Since the generator's real power is proportional to the slip, the mechanical speed is almost constant above the synchronous speed with small slip speed. The system is fairly simple, cost effective and robust when squirrel-cage induction generator is employed.

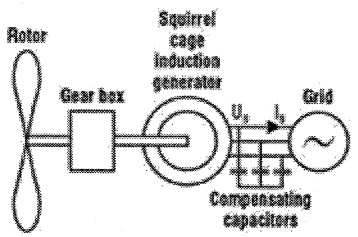

Figure 1-4 Fixed Speed Squirrel Cage Induction Generator

One of the drawbacks in the system is the reactive power. Undesirable reactive power is drawn from the grid under weak grid conditions, which further worse the grid system stability. Another major disadvantage is the power fluctuations seen in the output. When exposed to varying wind speeds, the input power varies with the wind speed cubic. Therefore the output power fluctuations are greatly influenced with the wind speed.

1.2.2 Variable Speed WECS

Unlike fixed-speed systems, the power electronic converter can be used in the variable speed system to minimize the power fluctuations as well as the reactive power compensation. The technology has been widely accepted in the wind energy industry. Variable speed systems, according to the types of generators, can be classified of synchronous generators, squirrel cage induction generators or wound rotor induction generators; Figure 1-5 illustrates the different categories of generators under each type.

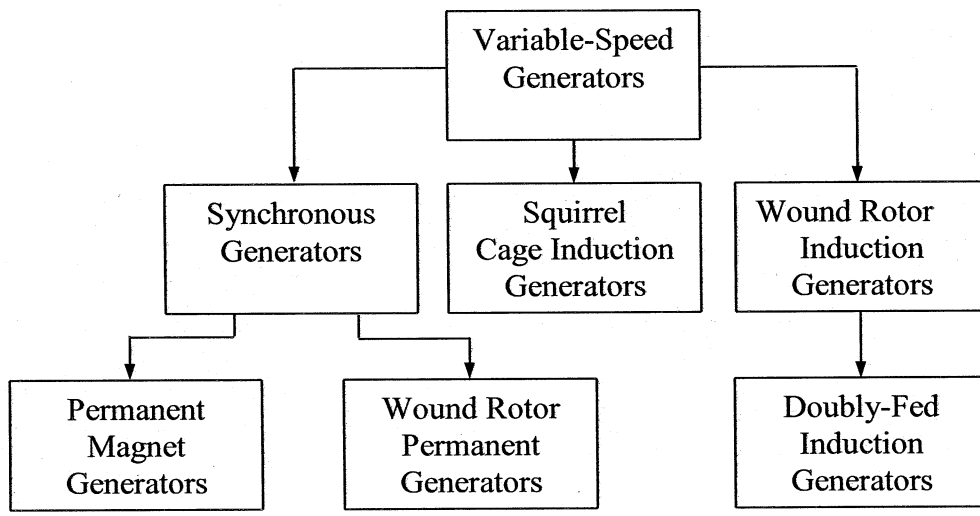

Figure 1-5 Variable Speed Induction Generators

As shown in Figure 1-6, a low speed direct-drive synchronous generator is connected to a full converter, which converts the variable voltage and variable frequency generator output to the fixed frequency and fixed voltage grid. The low speed generator, either electrical excited wound rotor or permanent magnetic, with large number of poles dramatically increases the size of the

generator. The advantages with this configuration are flexible active and reactive power control and high fault tolerance due to full scale power converter. Permanent magnetic generator has higher efficiency and less maintenance while wound rotor generator has the flexibility of excitation control. The power electronic converter involved in the power flow control becomes complex and costly because of the high power requirement for the converter.

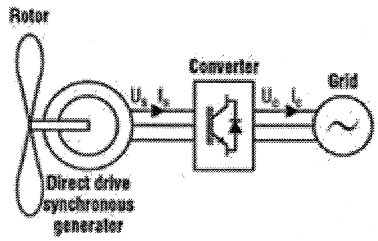

Figure 1-6 Synchronous Generator

1.2.3 Doubly-Fed Induction Generator

With the wide acceptation of wind energy in public, the need for large, robust and economical viable WECS is essential to meet the green power generation demand. Over the past ten years, the development of variable-speed systems, especially the doubly-fed induction generator (DFIG) based WECS has become increasingly popular for large scale utility level wind energy systems [5]. The apparent advantages of using the DFIG compared to traditional configuration already in existence are:

1) Variable speed operation with cheaper power electronic converter. The converter's rating is 25% to 30% of the total system power,

2) Lower harmonic distortion and low electromagnetic interference,

3) Flexible independent active and reactive power control [6],

4) Fast dynamic response of speed control.

As shown in Figure 1-7, the turbine rotor and generator shafts are coupled through a gearbox, converting the wind energy into electrical energy. The stator winding of DFIG is connected to the grid. A back-to-back converter exchanges the rotor (slip) power with fixed frequency fixed voltage grid to adjust the rotor speed. In practical applications a grid interface system consists of an isolation step-up transformer and LC filters for the converter.

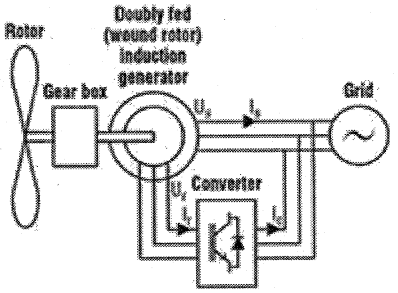

Figure 1-7 Wind Turbine System

The power electronic converter employed is a back-to-back converter consisted of two converters. Rotor side converter (or machine side converter) is connected to the slip rings and is responsible for controlling the torque, speed and power factor at the stator terminals. The stator side (or grid side converter) is connected directly to the utility and is used to exchange the energy between grid and DC link, keeping the DC Link voltage constant.

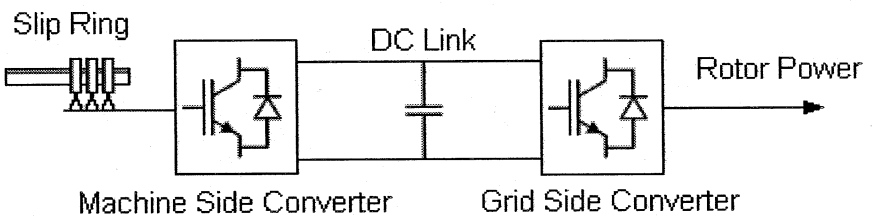

Figure 1-8 Back-to-back Converter

The generator speed can be lower or higher than the synchronous speed by supplying or extracting the slip energy from the rotor. The direction of the power flow is dependent on the operating mode which is defined as either, sub-synchronous or super-synchronous according to generator shaft speed. In Figure 1-9 both generating modes are illustrated in relation with the mechanical power, stator power and rotor power. Sub-synchronous generating mode occurs under such a slip conditions, where the stator provides power to the grid and the rotor consumes power. Similarly, super-synchronous generating mode is the opposite condition, when both the rotor and stator provide power to the grid.

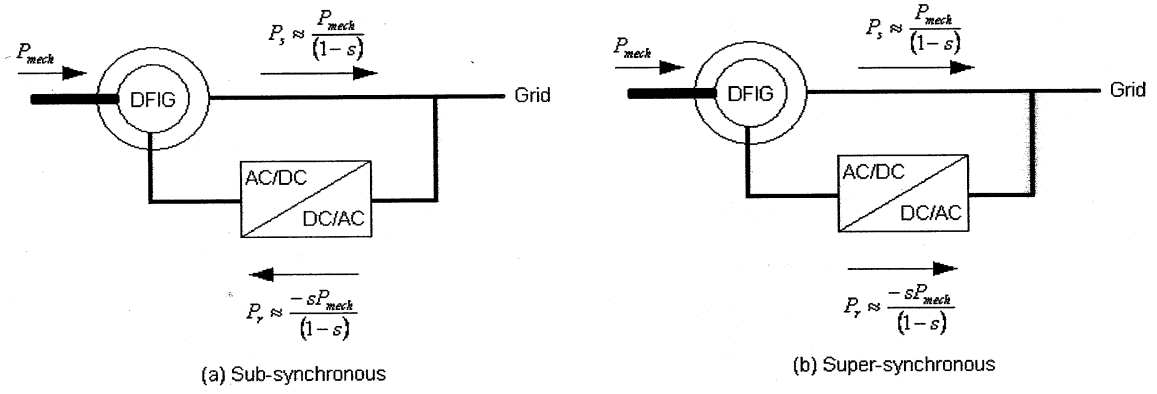

Figure 1-9 DFIG Power Flow Diagram

The control system was [7] developed based on field oriented control (FOC) theory which is ideal for stiff grid. Through FOC, the active power and reactive power from stator can be decoupled and independently controlled. Detailed explanation of FOC will be addressed in chapter 2.

1.3 Low Voltage Ride Through (LVRT) & Grid Connection Code

With large scale wind farms being commissioned, industry standards require wind generators to be treated in the same manner as traditional distributed generating systems. These systems are required to meet trip specifications, minor disturbances and support the grid under fault conditions. Industry leaders in wind energy technology are investing capital and research effort in addressing the issue of fault detection and the operation of there systems under grid disturbances. Tripping and reconnecting of large wind farm cause stability problems during faults, especially for a weak grid connection. Grid connection codes and power quality standards are driving forces for new installations, which force manufactures to design control systems with stringent tolerances and redundancy in anticipation of these faults. These systems should satisfy the requirements pertaining to frequency, voltage imbalances, voltage harmonics, outages, voltage variations, voltage dip, etc [8].

Faults imposed on the grid can occur anywhere within the connected system. Due to transmission line impedances the voltage dip could be seen at the stator windings. The voltage dip can cause excessive currents induced on the rotor windings by the magnetic coupling. As a

fail-safe mechanism, the DFIG automatically disconnects from the grid protecting the internal power electronic converter from over currents as well as over voltage on the converter dc link.

LVRT capability of WECS is usually defined by a non-trip area when the system terminal voltage falls in this area. As shown in Figure 1-10, the non-trip area consists of a minimums voltage and a slope of grid voltage recovery. The minimum voltage and duration is determined by the grid operator. Usually the duration lasts 10 to 20 cycles depending on different transmission conditions [9]. The width of the minimum voltage depends on the type of fault and the location at which the fault has occurred, the slope of voltage recovery is also determined by the interconnection strength between the grid and wind turbine system and the reactive power support [9]. There are many variations of the LVRT characteristic, however E.ON, the German Transmission and Distribution Utility has set the precedence of this requirement which can be simplified [10] as that the wind turbine should remain connected on-line during the fault while voltage at the point of connection drops to 15% of nominal (i.e. a drop of 85%) for a period of 150ms.

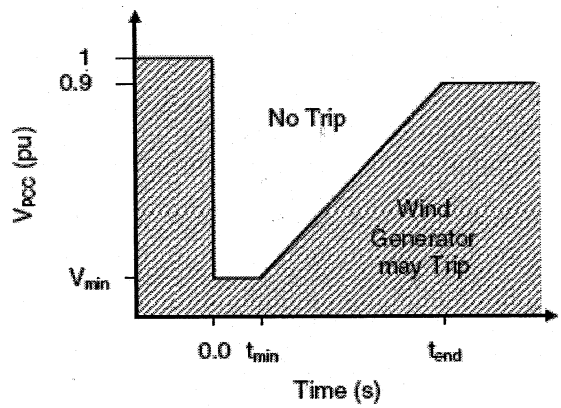

Figure 1-10 Typical LVRT Characteristic

Under fault conditions, there are two major problems for existing DFIG based wind energy system:

(i) Over current for rotor side converter and over voltage on dc link

(ii) Reconnection to recovered grid may cause stability issue.

Without a proper control scheme, DFIG induces large currents on the rotor side as the excitation current is low during faults. The generator flux is not maintained when the stator voltage drops

or negative rotating flux may appear if the system is severely unbalanced. It is desirable to regulate the terminal voltage (or reactive power) in order to achieve voltage stability and maintain a smooth voltage profile at the point of interconnection [11].

Upon fault recovery, the grid voltage increases to approximately 95% of the rated value however the grid is still considered to be very weak. Attempting to reconnect the WECS under this condition can cause the system to become unstable – as the WECS is being reconnected it pulls the grid voltage low due to reactive power. In practical applications, the WECS does not connect to the grid immediately after fault recovery. In fact reconnection only occurs once it has been determined the grid is stable enough. As the total installed capacity increases, frequency of re-connecting the wind turbines is not anticipated by system operator.

Traditionally the control algorithm internal to the wind turbine would have to be modified to incorporate fault detection and monitoring. In conjunction to the software, external hardware equipped to handle the fault operation under reduced supply voltage [9] must be appropriately selected for the application. The two most popular hardware solutions for solving the LVRT problem that have been researched and considered, include: (i) a power converter with UPS, the UPS behaves as a source or a sink allowing bi-directional power flow depending on the operation of the generator; (ii) active crowbar, power resistors are connected to the rotor windings and controlled to turn on absorbing excessive rotor energy. Table 1-1 summarizes additional LVRT alternatives. These techniques are all practical solutions however cost of implementation per kilowatt becomes a driving factor. Keep in mind that the cost may not be reflective of current semiconductor technologies therefore the cost breakdown is an illustration for comparisons purposes only.

Table 1-1 Summary of LVRT Alternatives [9]

LVRT Technology	Cost [$/kWatt]	Ride-Through Duration
Additional Capacitors	600	0.1 seconds
Boost Converter	100-200	5 seconds
Battery Backup	100-200	5 seconds, 1 hour
Super Capacitors	300-400	5 seconds
Active Crowbar	[1]	0.3 seconds

[1] Information is not available at the present time. The cost of the active crowbar solution would be very low.

1.4 Motivation

The proposed solutions listed in Section 1.3 are all applicable although the difficulty in system integration varies significantly. The energy storage option (such as back-up batteries, UPS and external converter topologies) is relatively complicated to implement in comparison to the other solutions, and the complexity of the control system housed inside the turbine increases. Depending on the operating mode of the turbine, a full power converter is required to supply enough power to DFIG through the rotor side, which dramatically increases the cost of the system Modifying the control scheme is also necessary in order to diagnosis the fault and protect the turbine under such grid faults. The energy storage solution is only good for a few hundred milliseconds after which time, severe damage could be incurred by the turbine if not disconnected from the grid sooner.

It is evident, under fault conditions, the converter is highly sensitive to excessive fault currents; an active crowbar is another method that provides an alternative current path for these currents whose magnitude exceeds the machine side converter ratings. The active crowbar is based on SCR controlled power resistors. The active crowbar can be a stand-alone system whose control scheme can be independent of the converter and controller system [12]. The research has been done for fault detection and active crow-bar protection system using rotor current which requires sensors mounted on the DFIG rotor windings. Current sensors are places on rotor windings and monitored for abnormal current profiles. The crow-bar would be activated when the rotor current exceeds the current limit. But this required the modification of existing system by adding additional hardware to the system. For protecting existing wind energy systems, which have been installed, a stand-alone active crowbar solution would be more attractive. In this solution, access to the rotor winding currents would be expensive, such that a new algorithm is needed to detect the fault.

This project proposes an alternative detection scheme for the active crowbar operation - the implementation of the active crowbar with integrated fault detection dependent only on the stator side voltage and DC Link voltage. The difference between the proposed system and the traditional active crowbar is the rotor current sensors. The intention of this project is to develop an alternative solution where the internal control of the wind turbine would remain unchanged and no additional current sensors would need to be installed inside the DFIG. In Figure 1-11, the

active crowbar is constructed using thyristors [6], which can tolerant high inrush current when the crow-bar is connected.

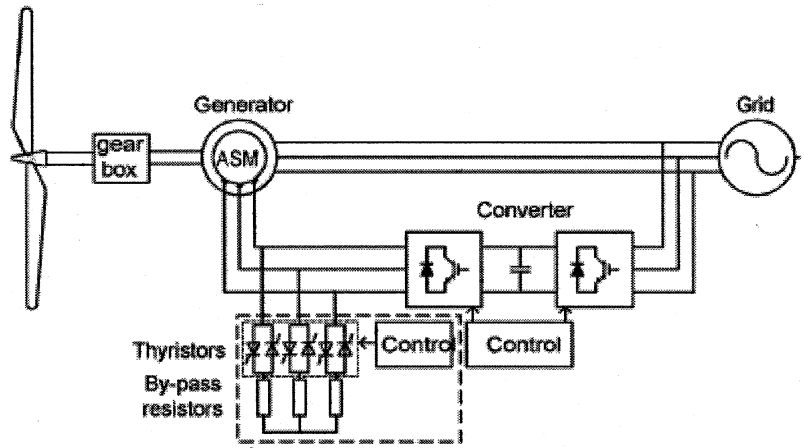

Figure 1-11 DFIG with Active Crowbar

Since the control scheme is dependent only on the stator side voltage and DC link voltage, these signals are manipulated using instantaneous pseudo-power detection to deduce the type of fault and take the appropriate course of action, in this case the machine side converter is disconnected from the rotor windings and the crowbar is activated. It is assumed that the pulse-width modulated signals (PWM) used to control the machine side converter is interfaced with an over-ride switch such that the converter can be disconnected under the introduction of a fault condition and reconnected after fault recovery.

The intent is focused on fault monitoring, detection and resolution in a wind turbine system. The behaviour of a single 1.5MW wind turbine system interconnected to the grid under various transmission level faults is investigated. These faults are categorized as either a single phase short to ground, three-phase short to ground and two phase short together or short to ground. Understanding system performance under this condition leads to the development of a complete active crowbar solution. As outlined in the grid connection code, the DFIG should stay online and satisfy the conditions of the LVRT characteristic for three-phase fault mitigation. The newly developed systems already incorporate the requirements in the internal controls. However this was not a consideration in the early year manufacturing of the turbines, therefore modifications are necessary in order to bring the system up to code.

1.5 Report Organization

In this report, Chapter 1 introduces the background of the wind energy system, grid connection code and motivation of this project. The report will be structured to provide more detailed information about the research done on the DFIG wind energy system, active crowbar and fault detection methods in the subsequent chapters.

Chapter 2 provides the theoretical explanation of the DFIG from the stator reference frame using equivalent circuit analysis. The field oriented control scheme is discussed to understand system implementation.

Chapter 3 deals with fault analysis, utility loading, grid stability and disturbances. The behaviour of the DFIG is analyzed under variable wind conditions and when faults are introduced into the system.

Chapter 4 presents the implementation strategy behind the active crowbar in Matlab/Simulink. Various control techniques are investigated and compared for fault detection and mitigation. System recovery is explained and simulation results of the wind turbine system with active crowbar verify the theory and proposed protection technique.

Chapter 5 provides an overview of the research undertaking, briefly summarizing the development of the active crowbar and control scheme, simulation results and major contributions to the field of engineering. Further research required is discussed.

CHAPTER 2 DFIG ANALYSIS

2.1 System Configuration

WECS main function is to convert the linear motion of the wind into rotational energy that can be used to drive the generator [9]. The maximum power extracted from the wind is achieved by adjusting the turbine rotor speed to the optimized value. Variable speed operation is obtained by injecting a variable voltage into the rotor at the slip frequency to adjust the slip power in the rotor [13]. In order to reduce the converter size, the slip power is limited such that DFIG based WECS has limited speed range. And it is very suitable for medium range wind speed. Under this condition, the power electronic converter are only required to handle a fraction of the turbine's total power, which is the slip power conducted through rotor slip rings. Losses can be significantly reduced compared to other generating systems with full power converter.

The system configuration is illustrated in Figure 2-1. The stator windings are directly connected to the grid. The grid also interfaces with the grid side voltage source converter (VSC) through filter. The rotor of the DFIG is equipped with three phase windings, which are supplied via the rotor side slip rings by a VSC of variable frequency and magnitude. Speed variation is ensured by the bi-directional transfer of slip power to the machine side converter [14]. Both the stator flux and rotor shaft are rotating at different speeds where the speed differential is related to the operating frequency of machine side converter. The machine side converter operates at the slip frequency, which is roughly proportional to the mechanical power input.

With the rotor circuit DFIG only responsible for handling 25 % to 30 % of the total system power while operating under a speed variation of ± 30% around the synchronous speed, lower rated power electronic devices results in lower losses and higher overall efficiency [13].

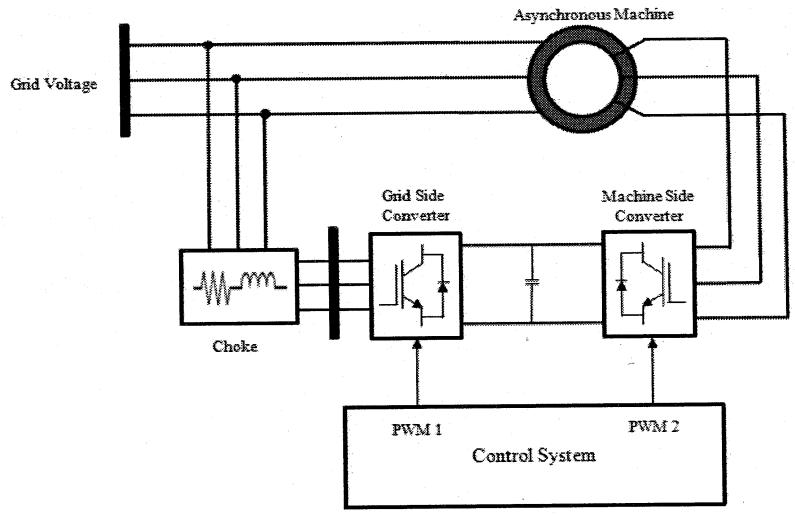

Figure 2-1 DFIG System Configuration

The grid side and machine side converter are controlled independently. The control system of the DFIG can be separated into three parts:

1) Speed Control is responsible for controlling the electrical power developed by the turbine by utilizing the MPPT characteristic, and pitch angle regulation.
2) Grid side converter control is responsible for regulating the DC link voltage meanwhile the active power converted by machine side converter is transferred to the grid side.
3) Machine side converter controls the rotor currents according to active and reactive power requirement.

The flexibility of controlling the power references independently provides a better grid performance enabling the wind turbine to act more as a dynamic power source [7].

2.1.1 AC/DC/AC Converter Topology

The back-to-back converter is based on a three phase voltage source converter topology where insulated gate bi-polar transistors (IGBTs) are popularly employed as the switching devices. The junction between the upper and lower set of switches per inverter leg is connected to either the grid for the grid side converter and to the rotor terminals for the machine side converter as shown in Figure 2-2. The diagram is a conceptual representation of the AC/DC/AC converter and does not include the line impedance or grid interface.

The control system is decoupled such that active and reactive power control is permitted. The flexibility in the control scheme allows for a flexible power flow control as well as the power factor is regulated.

The energy stored in the DC link capacitor is the difference between the power flowing to the grid and rotor power,

$$\frac{1}{2}C_{dc}\frac{d}{dt}v_{dc}^2 = -P_s - P_r \tag{2.1}$$

To sustain constant DC link voltage, a voltage regulator maintains a balanced power flow from the grid to rotor circuit.

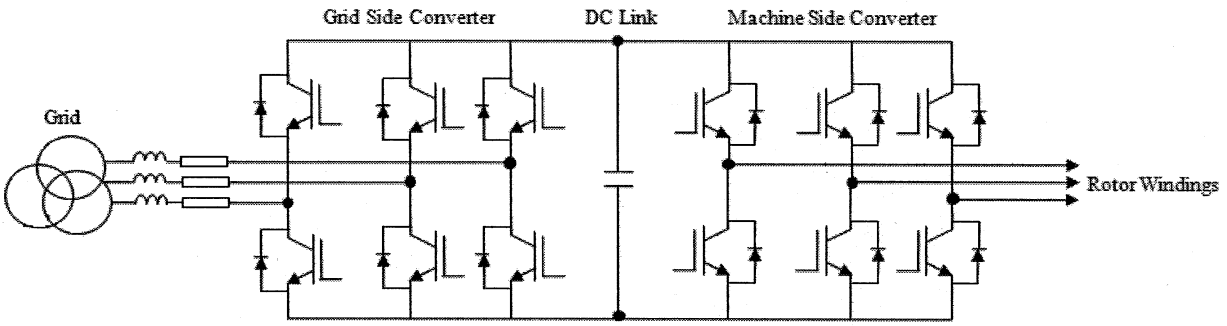

Figure 2-2 AC/DC/AC Converter

The subsequent sections will discuss in further detail the mathematical models and control algorithms for the entire system in order to fully understand the system operation.

2.2 DFIG Model and Control

2.2.1 DFIG Equivalent Mathematical Model

The *dq* reference frame was chosen to describe the equivalent circuit model where the stator and rotor variables have been decomposed using the Clarke-park transformation. The equivalent circuit of the DFIG with the exclusion of the magnetizing losses can be seen in Figure 2-3 [15]. The convention used to analyze the DFIG is generator reference frame, hence reference current is selected to supply active and reactive power to the grid.

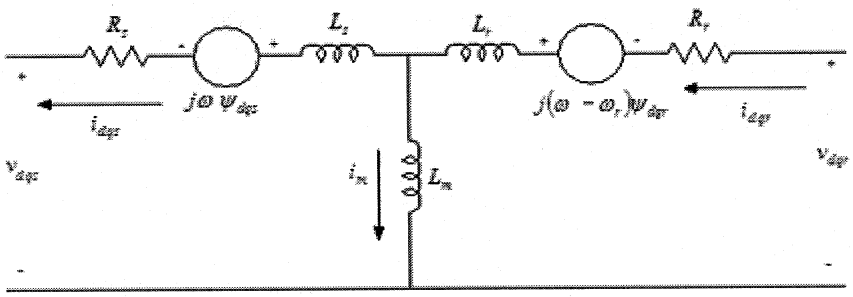

Figure 2-3 DFIG Equivalent Circuit

The DFIG can be represented by a fifth order [16] differential equations, applying Kirchoff's voltage law to the equivalent circuit shown in Figure 2-3, the following equations represent the stator and rotor voltage as a function of the magnetic flux.

$$
\begin{aligned}
v_{ds} &= -R_s i_{ds} - \omega_s \psi_{qs} + \frac{d\psi_{ds}}{dt} \\
v_{qs} &= -R_s i_{qs} + \omega_s \psi_{qs} + \frac{d\psi_{qs}}{dt} \\
v_{qr} &= -R_r i_{dr} - (\omega_s - \omega_r)\psi_{qr} + \frac{d\psi_{dr}}{dt} \\
v_{qr} &= -R_r i_{qr} + (\omega_s - \omega_r)\psi_{dr} + \frac{d\psi_{qr}}{dt}
\end{aligned}
\tag{2.1}
$$

The magnetic flux linkage is developed along the magnetic material when a current is flowing through the conductor. The flux linkage equations are represented in per unit and are described by Eqn (2.2).

$$
\begin{aligned}
\psi_{ds} &= -(L_s + L_m) i_{ds} - L_m i_{dr} \\
\psi_{qs} &= -(L_s + L_m) i_{qs} - L_m i_{qr} \\
\psi_{dr} &= -(L_r + L_m) i_{dr} - L_m i_{ds} \\
\psi_{qr} &= -(L_r + L_m) i_{qr} - L_m i_{qr}
\end{aligned}
\tag{2.2}
$$

Core losses are not considered in the mathematical model in order to simply the explanation. Substituting Eqn (2.2) into (2.1) results in a complex representation of the DFIG which illustrates the voltage-current relationship between the stator and rotor.

The direction of the rotor power is dependent on the operating mode of the DFIG. The rotor circuit absorbs a fraction of the power generated by the stator. Under super-synchronous

operating mode, if the stator generates 1.0 p.u. of active power at the rated slip, s, the total power delivered to the grid is (1.0 + s) p.u [17].

The rotation speed of the machine is in Eqn (2.3),

$$\omega_r = \omega_s(1-s) \tag{2.3}$$

The slip is proportional to the variation in the rotor resistance. Managing the energy in the rotor is achieved by providing a separate feed connecting the rotor windings to the machine side converter through slip rings.

The active and reactive power is described in Eqn (2.4),

$$\begin{aligned} P &= v_{ds}i_{ds} + v_{qs}i_{qs} + v_{dr}i_{dr} + v_{qr}i_{qr} \\ Q &= v_{qs}i_{ds} - v_{ds}i_{qs} + v_{qr}i_{dr} - v_{dr}i_{qr} \end{aligned} \tag{2.4}$$

The electromechanical torque, T_e a function of the rotor parameters and is directly influenced by the d-axis components, as shown in Eqn (2.5).

$$T_e = \psi_{dr}i_{qr} - \psi_{qr}i_{dr} \tag{2.5}$$

The change in generator speed can be determined using the generator Eqn (2.7) for motion, where the difference in input torque and electromagnetic torque causes the acceleration of the rotor.

$$\frac{d\omega}{dt} = \frac{1}{2H}(T_m - T_e) \tag{2.6}$$

The electromagnetic torque generated in the opposite direction to the mechanical torque applied to the turbine. If the turbine input torque is higher then the electromagnetic torque, the whole turbine/generator system will accelerate. The additional wind energy will be stored in the rotor as kinetic energy. This is the benefit of the variable speed system because the fluctuation in the wind energy is not transferred to the output power.

2.2.2 Machine Side Converter Control

The strategy of the machine side converter control scheme is based on the stator flux oriented control (FOC). This implies that the reference frame selected is aligned to the stator flux vector

of the DFIG; the stator flux reference frame is a synchronous frame, which rotates at synchronous speed. The current vectors are decomposed along this reference frame. Adjustment of the q-axis component of the rotor current controls the generator torque as well as the stator side active power of the DFIG [19]. The vector diagram of the DFIG is illustrated in Figure 2-4, where *e* denotes the synchronous frame and *s* denotes the stationary frame.

The stator flux vector in the stationary frame is denoted by λ_{dqs}^{s}. Eqn (2.7) shows the calculation of stator flux, where the flux linkages are calculated from the integral of electromotive force.

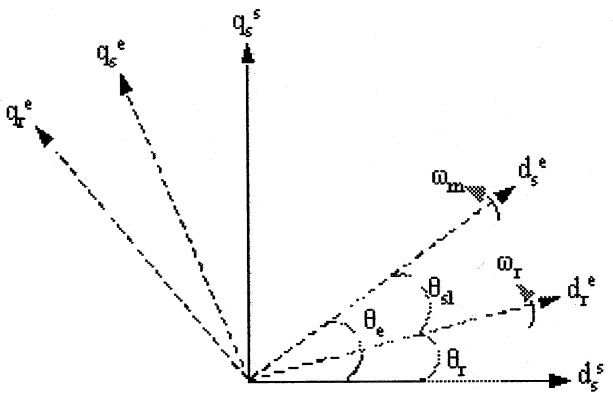

Figure 2-4 Vector Diagram of Stator Flux FOC

$$\lambda_{dqs}^{s} = \int \left(v_{dqs}^{s} - R_s i_{dqs}^{s} \right) dt \tag{2.7}$$

The angle θ_e is the tangential to the stator flux vectors giving the projection of the λ_{dqs} in the synchronous frame in Eqn (2.8),

$$\theta_e = \tan^{-1}\left(\frac{\lambda_{qs}^{s}}{\lambda_{ds}^{s}} \right) \tag{2.8}$$

From the discussion presented in section 2.2.1, the active and reactive power can be further simplified in Eqn (2.9) if only stator side power is considered. The rotor side power is exchanged by the converter, where active power and reactive can be fully controlled.

$$P_s = \frac{3}{2}\left(v_{ds} i_{ds} + v_{qs} i_{qs} \right) \tag{2.9}$$

$$Q_s = \frac{3}{2}\left(v_{qs} i_{ds} - v_{ds} i_{qs} \right)$$

With the d-axis oriented to the stator flux reference frame, the stator flux linkage, ψ_{qs} corresponds to,

$$\psi_{qs} = -L_s i_{qs} - L_m i_{qr} = 0 \tag{2.10}$$

Re-arranging Eqn (2.10) and $i_{qs} = -\left(L_m / L_s\right) i_{qr}$ illustrating the direct relation with i_{qr}. If the stator resistance is negligible, v_{ds} is zero. Therefore P_s can be re-written as [19],

$$P_s = -\frac{3}{2}\left(\frac{L_m}{L_s}\right) v_{qs} i_{qr} \tag{2.11}$$

The reactive power, Q_s is directly controlled by i_{dr}. The relationship between i_{ds} and i_{dr} is defined as a function of ψ_{ds} and the magnetizing current i_{ms}. The stator voltage is assumed to be constant, i_{ms} is almost a constant value. Therefore i_{ds} can be expressed in Eqn. (2.12),

$$i_{ds} = \frac{\psi_{ds} - L_m i_{dr}}{L_s} \tag{2.12}$$

In the selected reference frame, ψ_{ds} is equal to ψ_s , which is the product of the magnetizing current and machine inductance. Therefore, Q_s becomes,

$$Q_s = -\frac{3}{2}\left(\frac{L_m}{L_s}\right) v_{qs}\left(i_{ms} - i_{dr}\right) \tag{2.13}$$

It can be concluded that the machine side converter behaves as a controlled current source providing power control through rotor current regulations.

The implementation of the active and reactive power control is done by generating a reference current vector i_{dqr_ref} which is proportional to the reactive power reference, Q_{ref} and the torque command, T_e^*. From the derivation in Eqn (2.13), the reactive power is simply controlled by i_{dr}, since it is undesirable to supply reactive power to the grid, therefore Q_{ref} is set to zero and i_{dr_ref} compensates for reactive power consumption of the grid interface circuit.

In this project the input power is estimated from the wind turbine as the function of wind speed, rotor speed and pitch angle. The total electromagnetic power generated should be to maintain the speed at certain level and is calculated by deducting the mechanical losses and other losses associated. The stator side power is calculated from the electromagnetic power with subtracting

(or adding) the rotor side power and losses, including converter losses. The reference q-component of the rotor side current is then calculated from Eqn. (2.11). In real applications, as shown in Figure 2-5, a speed regulator is required to generate the reference torque since the power losses are difficult to be estimated. The speed regulator has a lower bandwidth and slow response. In the simulation the alternative approach employed is to generate the reference torque. The simulation speed can be improved in this manner.

The main function of the current regulator is to generate the proper voltage reference for tracking the reference currents, i_{dqr_ref}. The PWM signals are generated from the voltage reference. The current regulator is usually tuned to have a higher bandwidth which can be decoupled from the outer loop control.

To obtain independent control of the active and reactive power, it is essential all control variables are decomposed along the correct reference frame. Mutual flux linkage is estimated in Eqn.(2.14).

$$\lambda_{dqm} = L_s i_{dqs} + (i_{dqs} + i_{dqr}) L_m \tag{2.14}$$

Feed forward compensation is used to improve system dynamic response, V_{dq}^* is coupled with grid disturbances whose information is embedded in the stator voltage and flux linkage. The total reactance between the machine side converter and point of connection to the grid is determined [21], the contribution of this term is added to the V_{dq}^*. From Eqn. (2.15), the stator and rotor variables are cross-coupled through $L_m\omega_s$ and $(L_{lr}+L_m)\omega_s$ respectively.

$$V_{dq}^* = \left(K_p + \frac{K_i}{s}\right)(i_{dqr\_ref} - i_{dqr}) = R_r i_{dqr} \mp (L_{lr} + L_m)\omega_s i_{dqr} \mp L_m \omega_s i_{dqs} + v'_{dq} \tag{2.15}$$

The converter reference voltage is determined from Eqn. (2.15). The modulation index, m is determined by the DC link voltage as well as the magnitude of reference voltage.

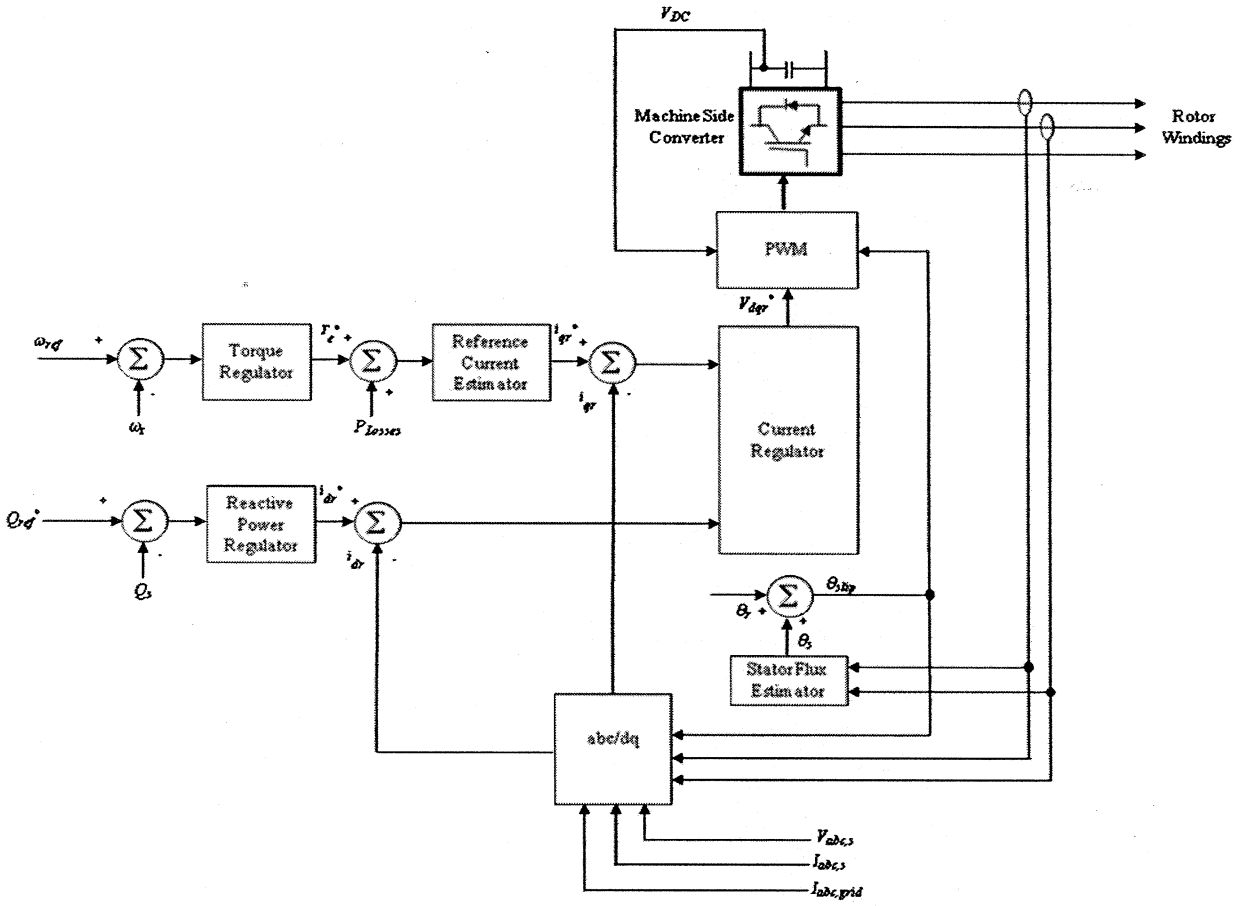

Figure 2-5 Machine Side Converter Control Block

$$m = \frac{2\sqrt{2/3}\left|V_{dq}^*\right|V_{nom}}{V_{DC}} \tag{2.16}$$

To implement the independent control, the rotor current and voltage are divided into components relating to the stator active and reactive power components [22]. The rotor current, i_{dqr} is aligned with the stator flux reference frame (where the stator flux is aligned to the d-axis). The torque and active power are directly controlled by i_{qr}. Since the machine flux is mainly determined by the stiff stator voltage, this enables the reactive power to be controlled by i_{dr} [23].

2.2.3 Grid Side Converter Control

The main purpose of the grid side converter is to establish a fixed DC link voltage regardless of the operation of the DFIG. The control scheme employed has been neatly presented in [41], this section will paraphrase the reference.

The rectifier performs the dual function of the boost converter and power flow regulation in the slip recovery. The converter circuit is modelled in Figure 2-6.

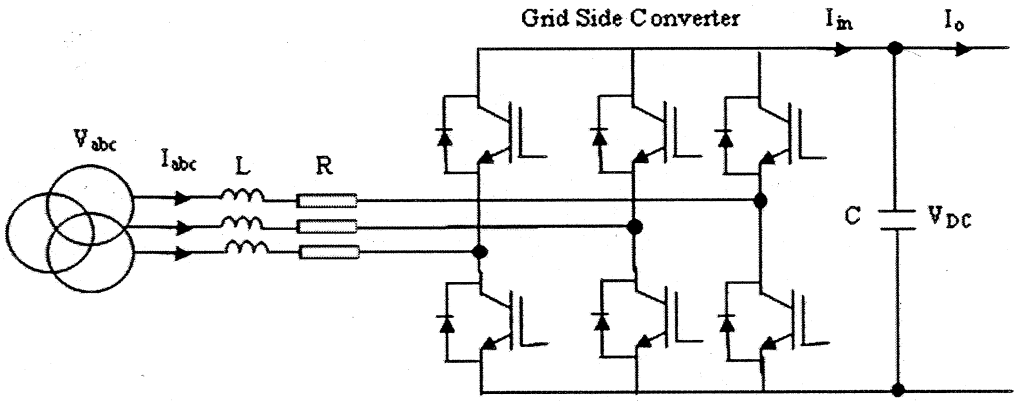

Figure 2-6 Grid Side Converter

The circuit is defined by the following set of Eqn. (2.17) in the synchronous *dq* reference frame.

$$\begin{bmatrix} v_d \\ v_q \end{bmatrix} = (R + sL) \cdot \begin{bmatrix} i_d \\ i_q \end{bmatrix} + \omega_e L \begin{bmatrix} -i_q \\ i_d \end{bmatrix} + \begin{bmatrix} V_d^* \\ V_q^* \end{bmatrix} \tag{2.17}$$

The total active and reactive power flows in the circuit described by Eqn (2.8). The general expression is assumed to be balanced and harmonic free.

The magnitude of the DC link voltage is clearly a function of the active power flow into the VSR. Assuming negligible switching losses, the power conversion law applied to the converter produces,

$$V_{DC} I_{in} = 3(v_d i_d) \tag{2.18}$$

The DC link voltage produced by the VSR is the function of the modulation index, *m* and supply line voltage, V_d. The expression in Eqn. (2.18) can be re-arranged and expanded to demonstrate

the DC link voltage is a function of i_d, the d-component of the supply current Eqn. (2.19) [20] and be controlled by an outer voltage control loop.

$$\frac{d}{dt}V_{DC} = \frac{1}{C}\left(\frac{3}{2\sqrt{2}}m \cdot i_d - I_o\right) \tag{2.19}$$

The equation in (2.19) can be easily represented using the first order linear system, while treating I_o as a disturbance which will be compensated for using a standard PI regulator.

The DC link control is expanded further to include an inner current control loop for proper measurement of I_{d_ref}. The control law for the current loop is relatively straightforward and can be described pictorially in Figure 2-7.

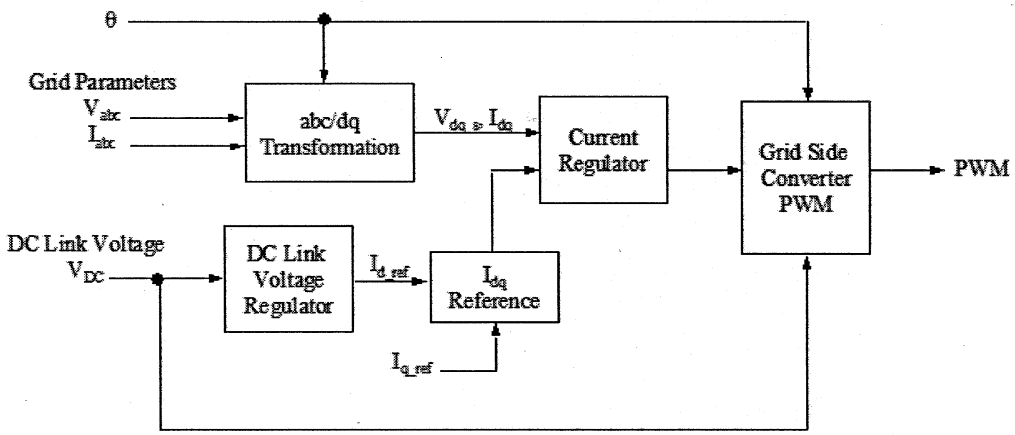

Figure 2-7 Grid Side Converter Control Block

2.3 Turbine Operation

Optimal tracking to provide maximum energy capture from the wind derives from the maximum power point tracking (MPPT) characteristic [20] illustrated in Figure 2-8. The tracking characteristic is specific for a desired turbine speed and optimal power output.

Because the DFIG control has limited speed range, at point A, the wind velocity is equal to the cut-in wind speed, typically 7m/s. Prior to point A, the turbine is off-line, the turbine will not

operate under 3m/s (cut-in wind speed) because the energy extracted by turbine is less than the system loss.

From point A to B, minimum rotor speed is developed, this usually is defined when wind speeds are low and the optimized speed is lower than the minimum operation speed. The machine side converter is operating at fractional power in this region of the curve.

Between points B to C, the maximum C_p is tracked maximizing the power captured from the wind. Operating in this region of the curve is optimal for tracking, the speed reference ω_{ref} is computed based on MPPT.

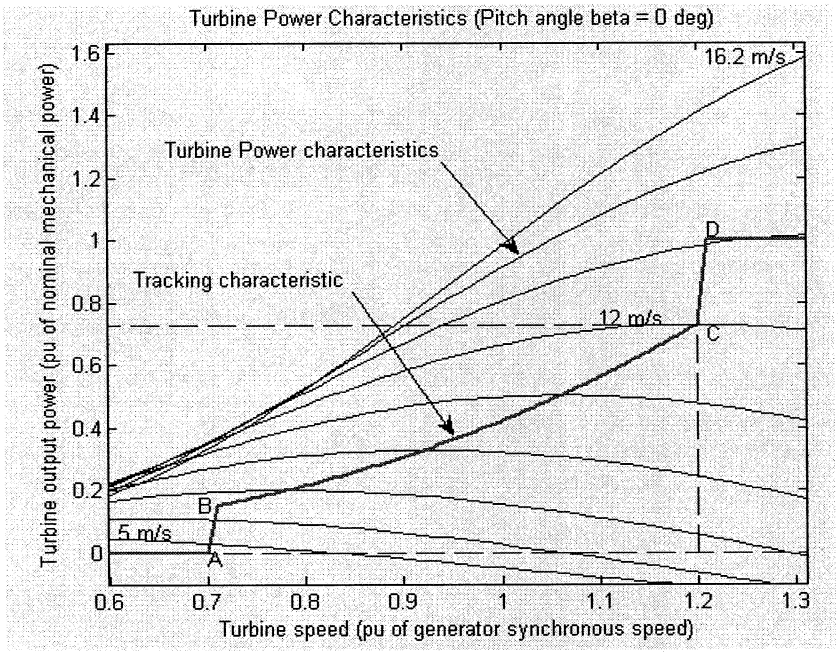

Figure 2-8 MPPT Characteristic

In this region of the MPPT, the pitch angle is zero degrees. From C to D, the maximum operating speed is reached such that the speed is limited and the power is increased to 1pu. At point D, the turbine is operating at constant power. If the wind speed increases such that turbine is operating beyond point D, above 1.2 p.u of the synchronous speed, the pitch angle regulator adjusts for higher speed wind variations such that turbine input power is limited. Even higher wind speeds will force the turbine to "cut-out", not to endure mechanical stress to the turbine and tower.

2.4 DFIG Normal Operation Analysis

In order to illustrate the control scheme and normal operation of DFIG based system, a single 1.5MVA wind turbine system with grid connection is modelled in MatLab/Simulink, shown in Figure 2-9. A 25kW collector transmission line (30km) connects the turbine output (through step-up transformer) to the transmission station. A 120KV/25kV transformer is used in the transmission station. Connected between the step-up transformer and generator output is a 500kW local load as well as a RC filter that absorbs transient spikes and noise.

The DFIG is modelled using a wound rotor asynchronous generator in the stationary frame where the stator and rotor windings are excited separately [1]. The generator is a three pole-pairs machine whose rotor windings are connected in Y-connection to an internal neutral point. The generator's parameters are listed in Table 2-1.

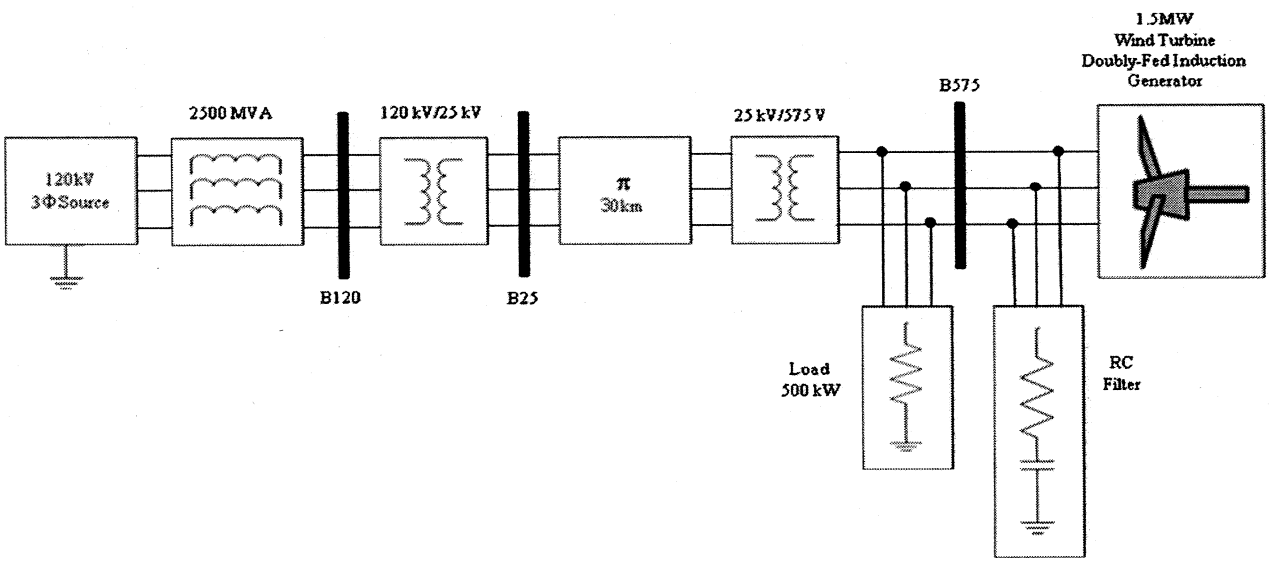

Figure 2-9 WECS Block Diagram

Table 2-1 DFIG Model Parameters

DFIG System Base Parameters	Values
System Power [MVA]	1.67
Nominal Voltage [V]	575
System Frequency [Hz]	60
DFIG Model Parameters	Parameter Values
Stator Resistance, R_s [p.u.]	0.00706
Rotor Resistance, R_r [p.u.]	0.005
Magnetization Inductance, L_m [p.u.]	2.9
Stator Leakage Inductance, L_s [p.u.]	0.171
Rotor Leakage Inductance, L_r [p.u.]	0.156
DC Link Voltage, V_{DC} [V]	1200
Inertia Constant [s]	5.04
Friction Factor [p.u.]	0.01
DC Link Capacitor [μF]	10,000
Nominal Line-to-Line Voltage[V_{LL},RMS]	575
Nominal Output Frequency[Hz]	60

The control block implemented in the DFIG subsystem is described sections 2.2 and 2.3. The stator voltage, stator current, rotor current, rotor speed and DC link voltage are sensed and fed to the controllers. The controller utilizes information provided by the wind turbine - the mechanical torque data is extracted and manipulated in the torque regulator producing the torque command. The grid voltage and reactive power are measured at the input terminals of the DFIG and fed to the controller as well. If Q_{ref} is set to zero, the WECS is operating at unity power factor.

Several regulators internal to the controller perform independent functions that are necessary for obtaining the desired output, they are:

1. Speed command uses the MPPT curve to build the speed reference and turbine output power. Torque command is extracted by estimating the stator side power.
2. Reactive power regulator is a close loop control whose feedback from the collector bus for power quality control.

3. Current regulator regulates the rotor current with respect to the reference value. The reference values are generated from torque command and the reactive power regulator.

The DFIG is equipped with line filters. The filtering function absorbs transients and acoustic noise generated by switching action of the power converter. The inductance of the filter is selected such that the current supplied to the grid meets the IEEE 519 [24] standard for low harmonic distortion

In real applications, the grid supplies current to the DC link capacitor charging it to the nominal rated voltage establishing steady state operation, the turbine then will begin to accelerate reaching the nominal rotor speed of 1 p.u. after which time the controller comes online. The initial transients seen in Figure 2-10 during start up are not an issue for a real application since the controller can limit the magnitude of rotor transient current. In the simulation, the initial conditions were set. These initial conditions attempt to replicate the real operation of the turbine, seen in the figures at time zero. The rotor speed does not start at 0 p.u. at time zero instead accelerates from a pre-set level of 1.1 p.u. The turbine in this project has a large moment of inertia, starting the simulation at zero rotor speed would require a very long ramp up time to steady state. Therefore the simulation was expedited to reach steady state faster.

At time zero the DC link voltage has a slight overshoot but quickly reaches the steady state value of 1200V. The voltage and current regulators are designed in a cascade fashion enabling the regulator to respond more quickly to disturbances and keeping the outer voltage control loop(s) and inner current control loop independent in there operation. This can be achieved because the current control loop has a higher bandwidth while the voltage regulator has lower bandwidth. Tuning is based on the phase margin of the overall control loop and bandwidth of the regulators. The selection of the bus voltage, reactive power and current regulator PI controller terms, K_p and K_i are summarized in Table 2-2.

Table 2-2 PI Controller Gain Terms

PI Controller	Proportional Gain, Kp	Integral Gain, Ki
Reactive Power Regulator	0.05	5.0
DC Bus Voltage Regulator	0.002	0.05
Grid Side Converter Current Regulator	2.5	500
Machine Side Converter Current Regulator	0.3	8

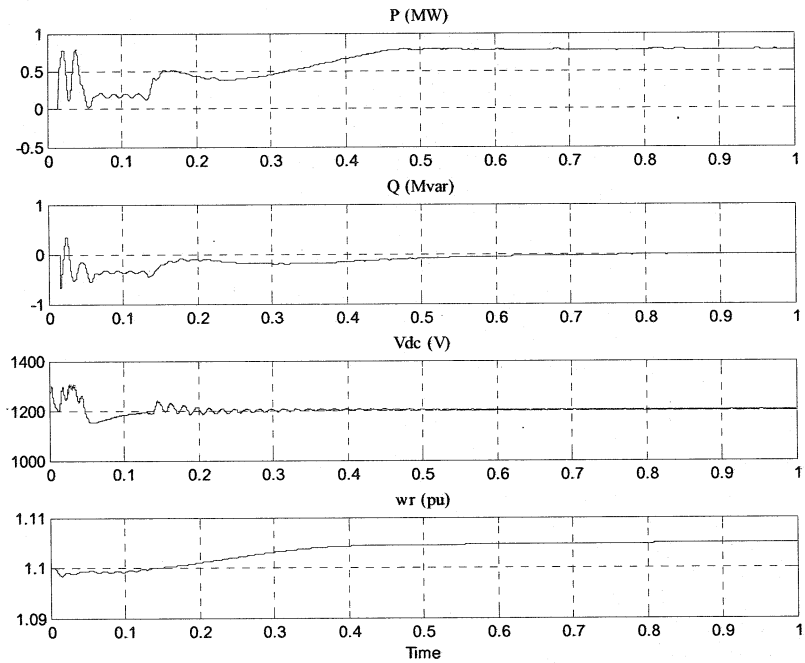

Figure 2-10 DFIG System Performance Characteristic

From Figure 2-10, the generator is operating in super-synchronous mode where the rotor is operating above the synchronous speed and the DC link voltage is maintained at the nominal value. The machine side converter operates at the slip power. The grid side converter regulates the power delivered to the grid causing the DC link voltage to decrease back to the nominal value.

The oscillations seen in Figure 2-11 are due to the initial condition of the stator flux not matching the actual stator flux. The only parameter that is controlled is the rotor current,

therefore during time 0 to 0.3 seconds the flux oscillates freely building up to the steady state value of 1 p.u. This phenomenon is reflected in i_{qr_ref} in the waveform above the flux magnitude plot. Once the flux oscillations cease i_{qr_ref} settles.

The derivation of the active power control scheme presented in section 2.2 supports the concept that i_{qr} is responsible for electrical torque control. Operating the DFIG at the rated torque fully energizes the rotor circuit. Minimizing the error between the i_{dr} and i_{dr_ref} reduces any flux differentiation.

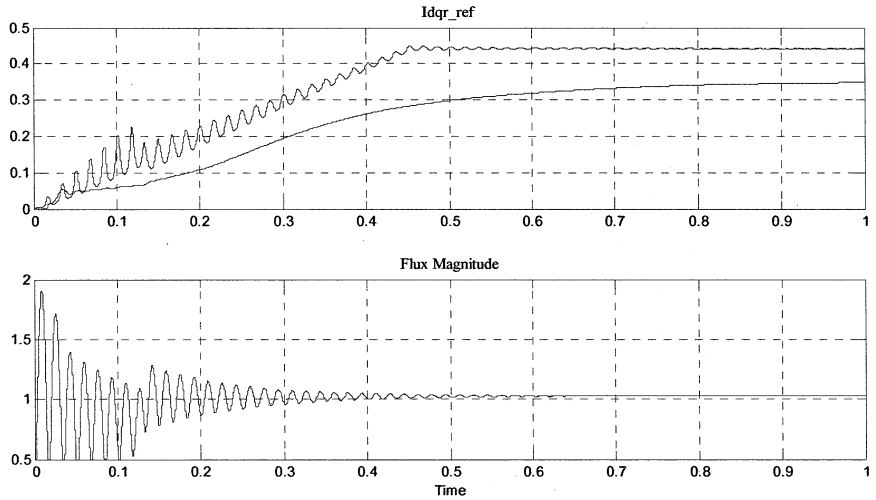

Figure 2-11 Rotor Reference Current and Stator Flux Magnitude

As the generator approaches steady state, the three phase rotor current in Figure 2-12 has a peak-to-peak value of 1.0 p.u. This figure clearly illustrates the machine side converter is only operating at fraction power.

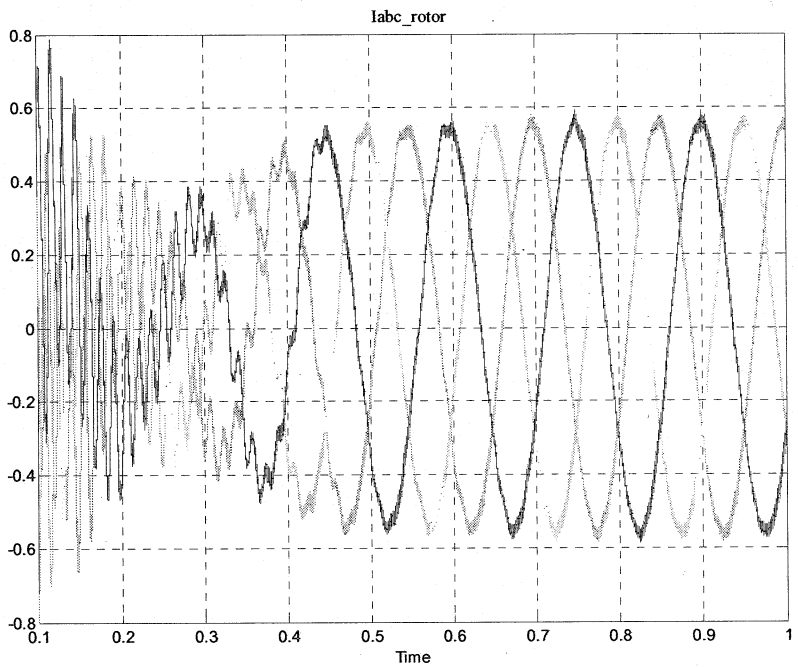

Figure 2-12 DFIG Rotor Current

2.5 Summary

The simulation of the WECS under normal operation verifies the theoretical operation and control of the DFIG. The stator active and reactive power control has proven to offer better system stability by means of decoupling the *d-q* components of the rotor current and controlling each power term separately. Power losses inherent to the turbine and feed forward compensation are realized in the control scheme providing more fast response. The rotor circuit only handles a fraction of the turbine power, therefore the switching devices in the machine side VSC are smaller contributing to lower overall system losses. Keeping the DC link voltage fixed allows for rotor slip power flow exchanged with grid. Finally the simulation results of the WECS supports the analysis presented in this chapter.

CHAPTER 3 ANALYSIS OF DFIG DURING FAULT

3.1 Introduction

With the increase of wind farms and offshore wind installations becoming the predominate means for power generation in many of the European countries, WECS like all power generating systems are required to meet grid connection codes guaranteeing compliance to the utility. Grid codes represent fundamental guidelines for wind turbine manufacturers and wind farm planners [14]. Here in North America, the grid connection code follows their European counterpart categorizing wind turbine capabilities as follows [25]:

(i) Low Voltage Ride-Through (LVRT) requirement to keep wind turbines on the grid during faults by introducing new technologies.

(ii) Even in case of tripping wind turbines have to guarantee reconnection and continuation of power generation in the shortest possible time.

(iii) The establishment of mechanisms for ascertaining and continuous monitoring of the fulfilment of grid requirements

(iv) Establishing intelligent system protection devices to ensure a minimum loss of wind power and to guarantee fast recovery of normal operation

In newer grid codes special requirements regarding voltage Total Harmonic Distortion (THD) levels in the Point of Common Coupling (PCC) as well as the ride through capabilities during fault events in the grid are specified. Moreover, the new wind turbines/farms should contribute to the regulation of active and reactive power and thereby contribute to the frequency and voltage control [26].

During grid disturbances the DFIG does not handle faults in the manner of conventional generator. The critical problems facing DFIG under fault conditions are the following: (i) rotor over current which can causes the machine side converter to be damaged or to be offline due to protection; (ii) DC link over-voltage which can lead to capacitor failure; (iii) temporary lose of control of the active and reactive power causing oscillations at the DFIG output; (iv) reactive

power compensation during voltage imbalance [27]. To avoid damage WECS were tripped offline, separating the turbine from the grid. Utilities are recognizing the need for WECS to withstand grid disturbances even if the voltage drops at the point of connection. These grid disturbances can either be classified as balanced or unbalanced. Depending upon the network configuration and WECS topology, the turbine may experience different situations at the turbine input terminals. To avoid voltage collapse, the grid requires intelligent protection schemes which can handle fault conditions in a shorter duration. This topic will be discussed in the next chapter.

In this project, short circuit faults are considered in the simulation. These faults are imposed along the transmission line and are categorized either as shorted phase(s) to ground or arching between phases. The simulation analyzes the behaviour of the DFIG under each fault condition (under constant wind speed) and the undesirable fault response characteristics will be observed in the large peak currents at the initiation of the fault and uncontrollable active and reactive power generation and consumption [27].

3.2 DFIG during Fault

In the simulation, the fault condition is introduced into the system at 0.4 seconds when the DFIG enters steady-state and removed after 0.7 seconds allowing the DFIG to recover to steady state.

3.2.1 Three Phase Shorted to Ground

A three phase fault is considered as a balanced fault condition as all three phases experience the same grid disturbance. For a more realistic representation of a three phase short to ground, the fault was induced far from the wind energy system. A theoretical short to ground is one in which is represented by zero impedance however in a practical environment the ground impedance is a few milliohms causing power losses as a result of circulating ground currents. Similarly the voltage seen at the output of the DFIG will differ from the grid voltage at the location of the fault due to transformer and line impedances. Figure 3-1 shows the simulation results of three-phase fault.

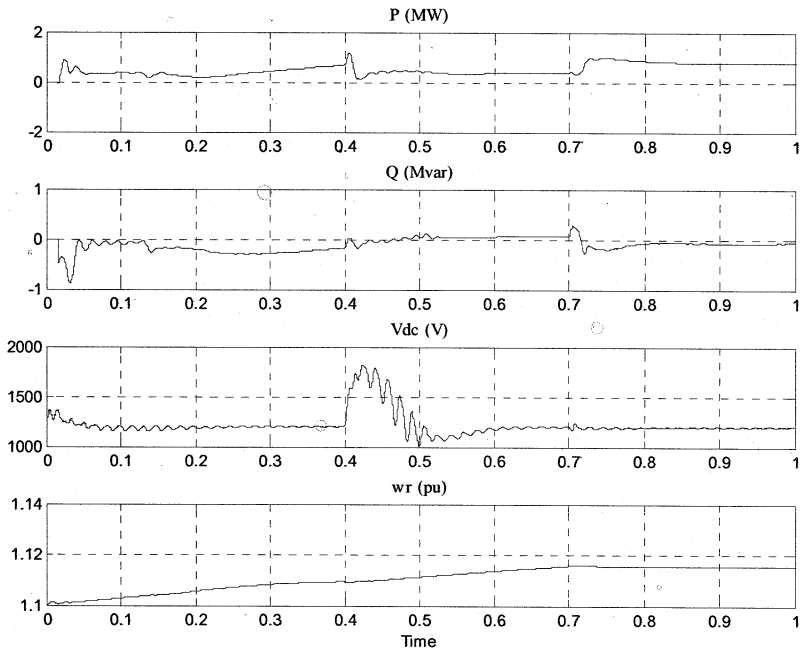

Figure 3-1 DFIG Characteristics under 3ϕ Fault

At the instant the fault is introduced into the system, the DFIG input voltage observed at B575 collector bus becomes out of phase with respect to each other. The active power *P* decreases to 0.36 p.u. as a result of the ground impedance. From the discussions regarding the reactive power control in section 2.0, the changes are insignificant compared to the active power characteristic. The reactive power, *Q* can be maintained. The FOC implemented is designed to keep the reactive power at zero.

Before the fault is introduced into the system, the DC link voltage has a steady state value of 1200V containing a small AC ripple. During the fault initiation, the capacitor voltage increases above its rated value to a peak value of approximately 2000V, shown in Figure 3-1. Large rotor currents shown in Figure 3-3 is induced exceeding the nominal value of 1.0 p.u. in the rotor windings from the stator increasing this voltage across the DC Link capacitor. Even the duration of the peak voltage does not last very long as the voltage regulator at the grid side brings voltage back to the nominal value, the voltage is still much higher than the capacitor and switching device break down voltage, causes the failure of the system if there's no protection.

The voltage sag has a significant impact on the rotor current. There are two transient procedures during the fault. First the rotor voltage decreases to a minimum and the machine side converter loses control of the rotor current. The current reaches very high peak and DC link voltage increases to a maximum. Then the controller gains the control capability when the DC link voltage decreases. It is expected that the transient rotor current exceeds two to three times the rated value as the grid voltage decreases more then 80%. The rotor power developed during this stage is transferred to the DC link capacitor which can increase beyond 250% of the nominal rotor power [28]. The large developed rotor power needs to be addressed since the power electronic converter is only rated for a fraction of the total turbine power.

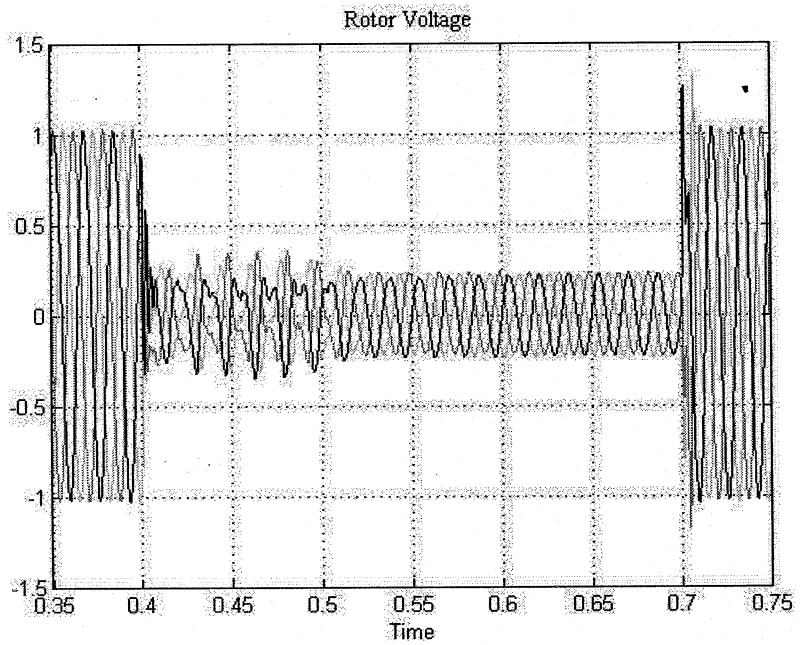

Figure 3-2 Rotor Voltage

Due to the integrated control system of the DFIG, the grid side converter attempts to stabilize the DC link voltage. The grid side converter current increases up to 50% of the wind turbine nominal current representing an overload condition [14]. Protecting the grid side converter from fault current isn't critical since the converter may still be within the device rating to handle such an overload.

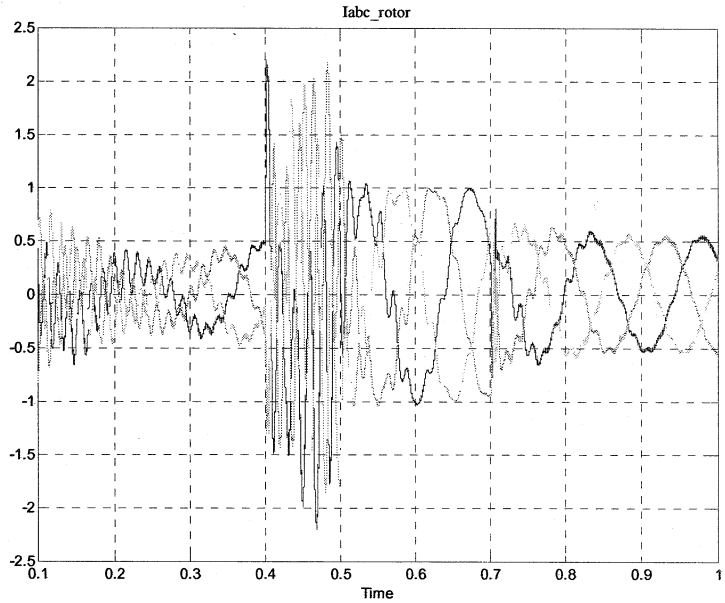

Figure 3-3 Rotor Current under 3ϕ Fault Condition

It is evident from the observations made above, the DC link over voltage and excesses rotor current developed at the machine side converter can be alleviated by means of removing the machine side converter out of the DFIG system and shorting the rotor terminals by external circuit. The protection algorithm should monitor and provide fault mitigation action when the wind energy system is experiencing a balanced fault condition.

3.2.2 Single Phase Shorted to Ground

A single phase fault is simulated in the same location as the three phase fault, where only one phase is shorted to ground. Most mega-watt electric systems can handle single phase faults as they pose no immediate threat to the generating system. The simulation results are shown in Figure 3-3. With the unbalanced voltage, large rotor currents are induced in the rotor windings almost exceeding 1.0 p.u , which exceeds the converter ratings.

The active power *P* remains unchanged at 0.8 p.u during the fault. However after the fault, the active power decreases slightly. The same phenomena can be observed in the rotor speed, where the DFIG is operating above the synchronous speed.

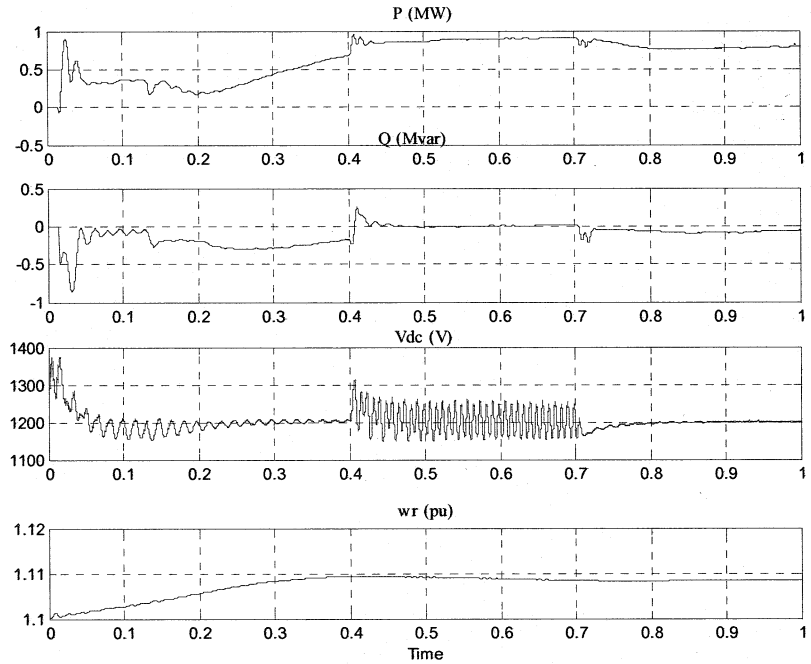

Figure 3-4 DFIG Characteristics under Single Phase Short Condition

As shown in Figure 3-4, the DC link voltage doesn't vary much from the reference value of 1200V. However a noticeable 120Hz AC ripple is imposed on DC link voltage. The voltage imbalance induces a negative sequence component which can be seen both on the DC link voltage and the rotor current at 120Hz, as shown in Figure 3-5. The low frequency 120Hz component charges the dc link capacitor, which causes the ac ripple. Because the DC link voltage is still within the nominal operating limits set in the regulator, the ripple goes undetected.

Single phase faults pose a serious problem to the DFIG, the not so obvious rotor over current puts the entire system under considerable stress. Despite the fact the DFIG can still operate under unbalanced faults, this is not recommended.

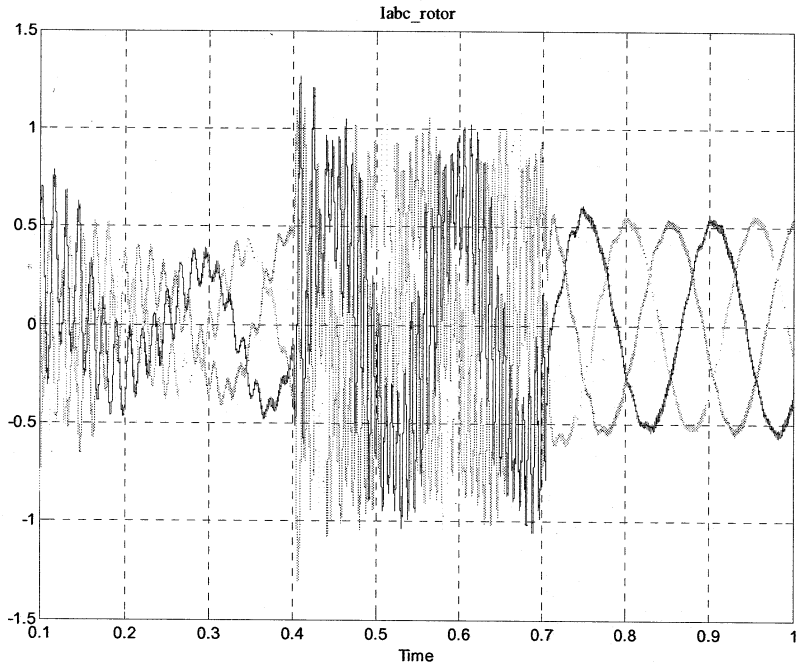

Figure 3-5 Rotor Current under Single Phase Short Condition

3.2.3 Two Phase Shorted

Unbalanced fault conditions are severe in nature and need to be addressed in the similar manner as balanced faults. Two phases shorted together or shorted to ground is more serious than single phase faults. From Figure 3-6, the reactive power Q spikes as the fault is applied and removed from the system. Since the reactive power regulation is set to zero, reactive power is drawn from the grid in attempt to compensate for the voltage sag at the input of the DFIG.

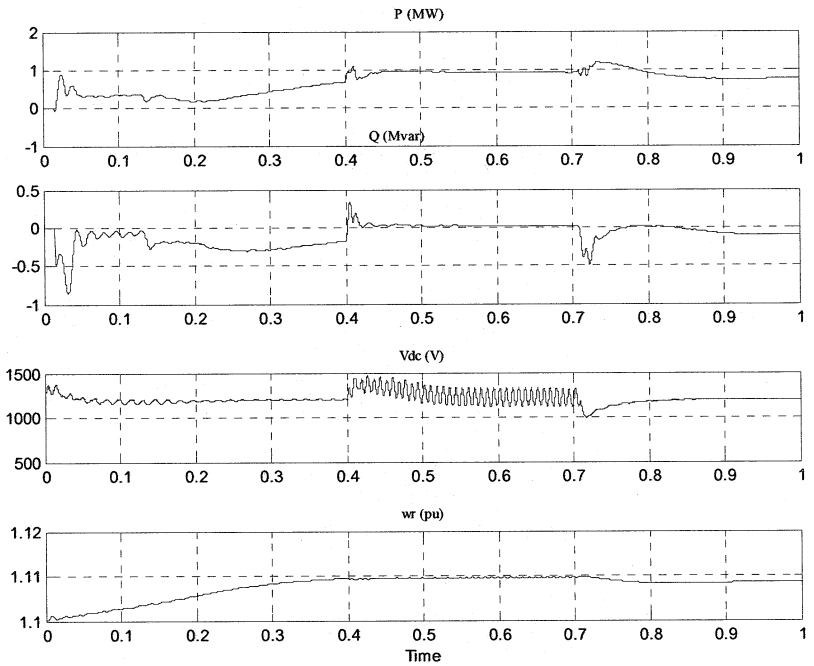

Figure 3-6 DFIG Characteristic under Two Phase Fault Condition

As with the single phase fault, the negative sequencing component is seen in both the DC link voltage and the rotor current. The magnitude of the rotor current under an unbalanced fault condition is almost twice the rated value lasting the entire duration of the fault. Due to the voltage imbalance a negative sequencing component is imposed on the rotor current whose frequency is the addition of the slip frequency plus twice the fundamental frequency of the DFIG. Therefore an around 120Hz component can be seen in the rotor current. The positive sequence component is reflected in the slip frequency therefore detecting only the negative sequence component encompasses this characteristics. Similarly, the zero sequence component is of no interest as this characteristic is inherent only to the stator circuit which does not have severe effects on the grid side power converter [27].

We see in Figure 3-7, the rotor current is three times the nominal value, much higher then the rotor current measured during a single phase fault. This supports the need to detect and mitigate against unbalanced fault conditions.

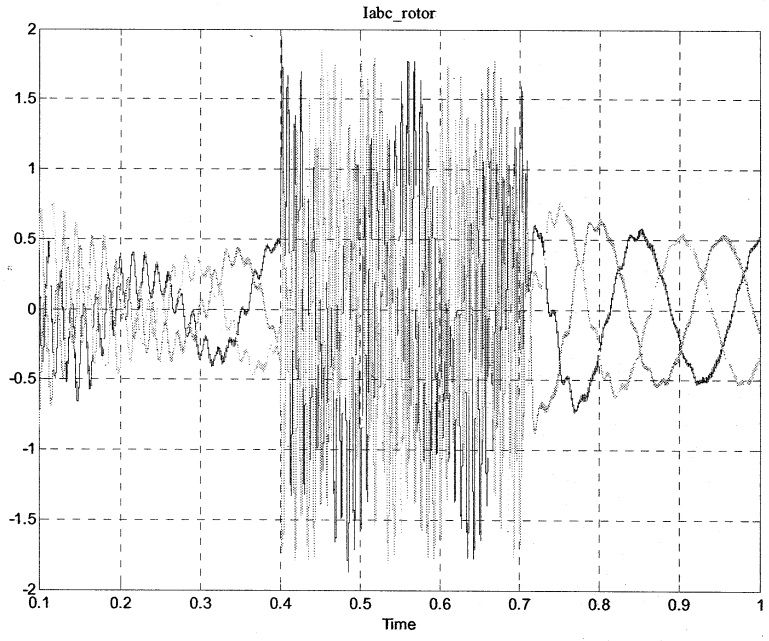

Figure 3-7 Rotor Current under Two Phase Fault Condition

3.3 Summary

From the analysis present in this chapter, it is evident each type of grid disturbance has inherent characteristics that can be utilized in a detection scheme. In this chapter, three typical types of faults are imposed to the DFIG. The simulation results are analyzed. The machine side converter operates over rating during fault, which may cause severe damage to the converter or cause the system protection to trip the WECS off grid. The fault detection method for each type can be summarized by the following:

For balanced fault conditions, the large induced current on rotor side is transferred to the DC link capacitor. The DC link voltage increases beyond the capacitor's rating before the DFIG voltage regulator can control this parameter. The impact of the low voltage causes the rotor current to increase 2 to 3 times the rated value in order to compensate for the flux reduction. Due to the extremity of a three phase fault, monitoring the magnitude of the collector bus voltage and converter dc link voltage will annunciate this type of fault.

In the cases of unbalance faults, the voltage imbalance impacts the performance of the DFIG. A negative sequence component (around 120Hz) is imposed in both the rotor current and DC link voltage. Since the DC link voltage meets the regulation limits internal to the DFIG control scheme, detecting the dc link voltage is not ideal to determine the fault. More over, the faults can be reflected in the stator phase voltage. Keeping with the proposed detection method outlined in Chapter 1, using only the stator voltage to deduce the pseudo-active and reactive power terms keeps the protection system independent from the DFIG control even during unbalanced fault conditions.

CHAPTER 4 FAULT DETECTION

4.1 Fault Introduction

The behaviour of the DFIG under normal and fault operating conditions under constant wind speed has been analyzed. The power electronic converter responses to different fault conditions were conducted where the rotor side currents exceed the converter rating. The traditional approach of protecting the wind turbine and grid during fault conditions was to trip the generator off-line and reconnect only after the fault is removed and the grid voltage is stable enough to handle the reconnection – as a precaution not to depilate the grid further by reconnecting under unstable voltage condition. Having the wind turbine trip off-line has a significant impact on the overall generating resource, especially when the wind energy penetration is high in some area.

As mentioned in Chapter 1, the penetration of wind energy could reach 20% in some European countries. Large scale wind farms can not be allowed to trip off-line under such fault conditions. Another problem that needs to be considered is reconnection. Reconnection of a single turbine to the grid may not a big problem, however reconnecting an entire wind farm to the grid could have significant negative impacts, such as excessively large transient voltage and frequency. The wind energy is not predictable and controllable, which is also a problem for reconnection to the grid.

Many different approaches have been investigated that solve the fault ride-through problem and keep the turbine on-line under fault conditions. The technique, which is employed in this project is the active crowbar. This system is designed to short the rotor windings during fault condition such that excessive rotor current will be dissipated across a passive device. And the fractional power converter is disabled by the gating signal.

The following sections will discuss different active crowbar configurations, the fault detection method, the integration of the active crowbar system with the DFIG and the overall system behaviour under various fault conditions.

4.2 Active Crowbar

The idea of using crowbar is to provide a bypass path for high rotor current during fault conditions. This can be achieved by, shorting the rotor windings and disconnecting the machine side converter ensuring excessive current is not transferred to the DC bus.

The configuration of the active crowbar varies amongst many of the research papers. The typical configuration is based on a three-phase rectifier whose output is connected through a switch (thyristor) to a resistive load [29]. The resistance of the load is determined by the excessive current during fault condition. The value should be selected such that it is small enough not to induced a large voltage at the converter input terminals but large enough to limit the current [6]. The switch used here is thyristor, which has high transient current capability, simplified gating circuit and reduced cost.

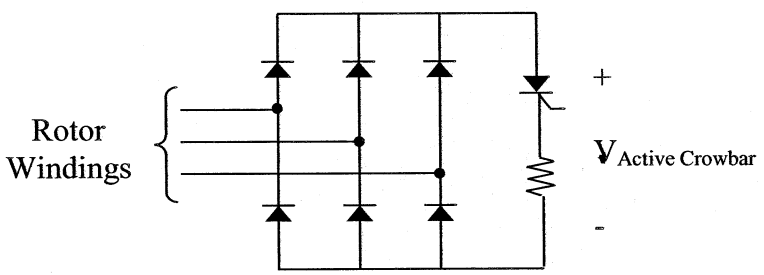

Figure 4-1 Active Crowbar – Rectifier Configuration

The thyristor in Figure 4-1 will be on until the fault is removed. Force commutation is required to deactivate the thyristor and resume the machine side converter. To the contrary, the active crowbar configuration in Figure 4-2 is based on the concept of the AC switch and does not require force commutation circuit to turn off the thyristors. Only current signals are injected to the gate, turning on the devices. Turn off of thyristors can be done by natural commutation. This configuration requires simpler control but is more costly to implement since the number of switching devices has increased to six.

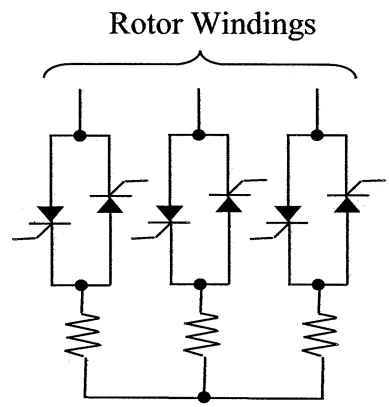

Figure 4-2 Active Crowbar – Thyristor Configuration

The cost savings tied to an active crowbar is dependent on the complexity of the configuration. type of semiconductor devices used, and control scheme required. Size of the unit and manufacturability are factors that also need to be considered when developing a stand-alone system. Space is limited inside the wind turbine's hub therefore optimizing the design is a driving factor in the overall protection scheme.

For the active crowbar to be effective, the machine side converter is disabled at the instant the fault is detected. Additional circuitry embedded in the fault detection provides the means of disabling the PWM gating signals from the converter.

In the simulation, the rotor windings are simply shorted through circuit breakers, which is idealized device of anti-paralleled connected thyristors. The resistance, which dissipating the excessive rotor energy is include in the circuit breaker as the internal impedance.

4.3 Fault Detection Methods

The fault detection method investigated in this project plays an important role in the independent active crowbar system. The active crowbar is connected to the rotor windings providing a bypass path for the rotor current under critical fault conditions. This section will focus on the detection rather then active crowbar hardware,

The system configuration of the DFIG with active crowbar connected is illustrated in Figure 4-3. Additional circuitry is required to disable the machine side converter gating pattern in turn removing the machine side converter from the DFIG system.

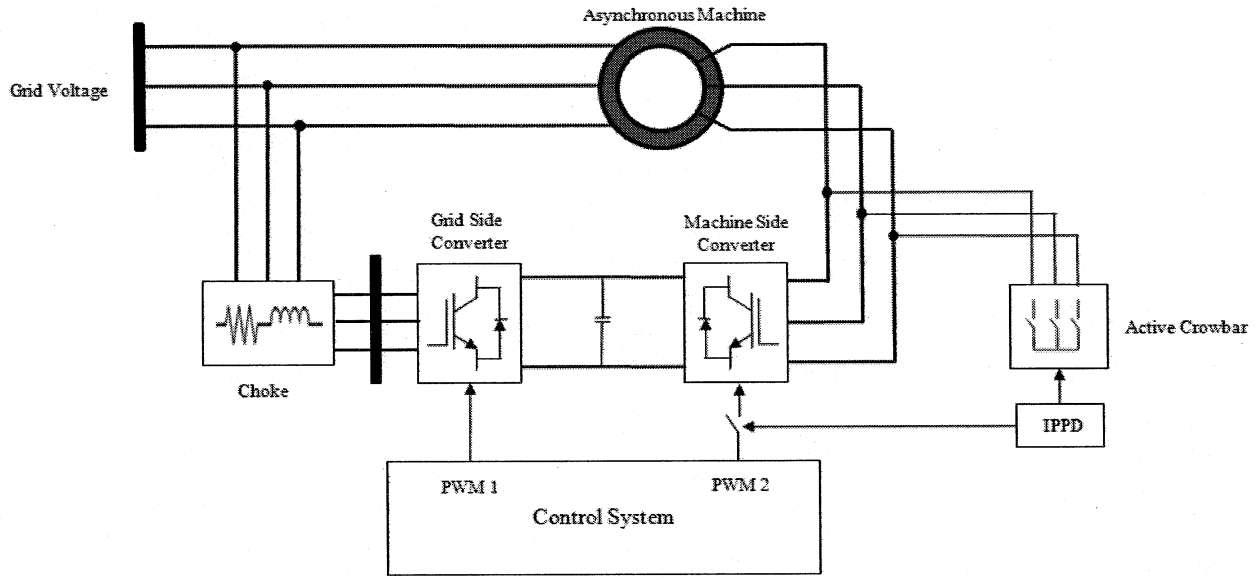

Figure 4-3 DFIG with Active Crowbar Protection System

Several detection methods were investigated to detect single, two and three phases faults and provide real-time signal to activate the crowbar. Two out of the three methods do not provide instantaneous response, therefore high transient current or over voltage may be seen on the machine side converter. In this section, several methods are compared and a suitable method is proposed.

4.3.1 Fault Detection using Rotor Current

Under fault conditions, the rotor current exceeds the converter rating substantially, which can be used for fault detection. The three-phase rotor currents are sensed and feed into the detection block, where the currents are converted to the *dq* reference frame to have a faster response. The magnitude of current vector is compared to a reference value and fault indication is latched based on the equality.

$$I_{rotor,abc}\begin{cases}\leq 0.5 p.u, \textit{normal operation}\\ \geq k\cdot 0.5 p.u, \textit{fault}\end{cases} \tag{4.1}$$

where k is the overload factor, 120% *to* 150%

Under normal operating conditions, the nominal maximum rotor current is approximately 0.5 p.u using the equality describe in Eqn. (4.1), the instantaneous rotor current exceeds 120% to 150% of the nominal value, the crowbar is activated. This margin is determined by the converter design criteria – typically the converter can tolerate 120% to 150% of converter rating depending on different design and applications.

In theory, this technique is very suitable for converter protection rather that the ride-through because it directly addresses the problems related to the converter. However, accessing the rotor side current after the turbine is manufactured is not easy and can become quite costly. The addition of two current sensors adds to the hardware and can introduce singe-point failures during the installation.

From a controls perspective, differentiating among different types of faults is complicated. Therefore the control algorithm will become more complex when using the rotor current as the primary means for fault detection.

4.3.2 Fault Detection using Voltage RMS Value of Stator Voltage

This rotor current detection technique is expensive for a standalone crowbar. Fault usually appears as the voltage dip on the stator side. Then the stator voltages can be used to detect the fault. This method segregates the active crowbar independent from the turbine's control system.

The stator phase voltage is sensed and then the cycle RMS value of the phase voltage is computed. The RMS values of voltages are compared to a predefined threshold value. The fault status is latched and can only be reset after the fault is removed. The RMS value of a continuous periodical function, in this case the stator voltage, can be approximated by computing through one cycle as shown in Eqn (4.1).

$$f_{rms} = \sqrt{\frac{1}{T_{n+1} - T_n} \int_{T_n}^{T_{n+1}} [f(x)]^2 dx} \tag{4.1}$$

The issue about the RMS calculation is the time delay in the response: A one cycle time delay is introduced in the fault detection, therefore the response is not instantaneous, but depends on the cycle duration, excessive rotor currents can still damage the power electronics device if the converter has low tolerance of the over current.

The block diagram in Figure 4-4 shows the implementation of the detection of using RMS value of voltage. The gain block multiples each phase of the stator RMS voltage with a predefined constant value, *K*, that define the upper and lower boundaries of each type of fault – three phase short to ground, single phase short to ground and two phases shorted together or to ground respectively.

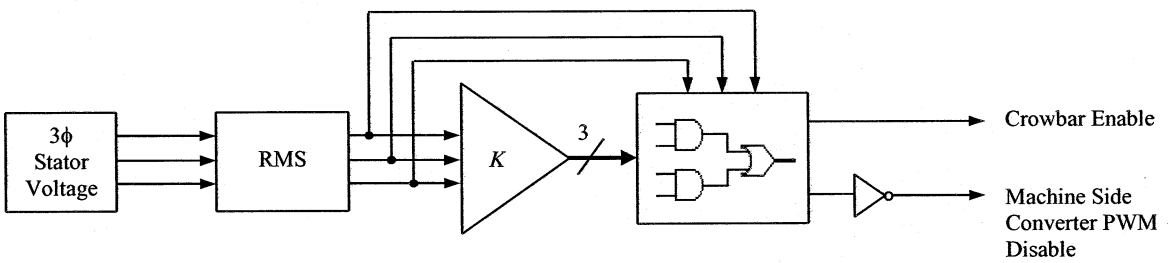

Figure 4-4 Mean Value Theorem Control Block

The simulation results in Figure 4-5, illustrate the impact of the cycle delay on the rotor current. The three phase fault is introduced at 0.4s however the crowbar control algorithm responds at 0.416s, during this time, the rotor current exceeds its nominal value and reaches 1.0 p.u.

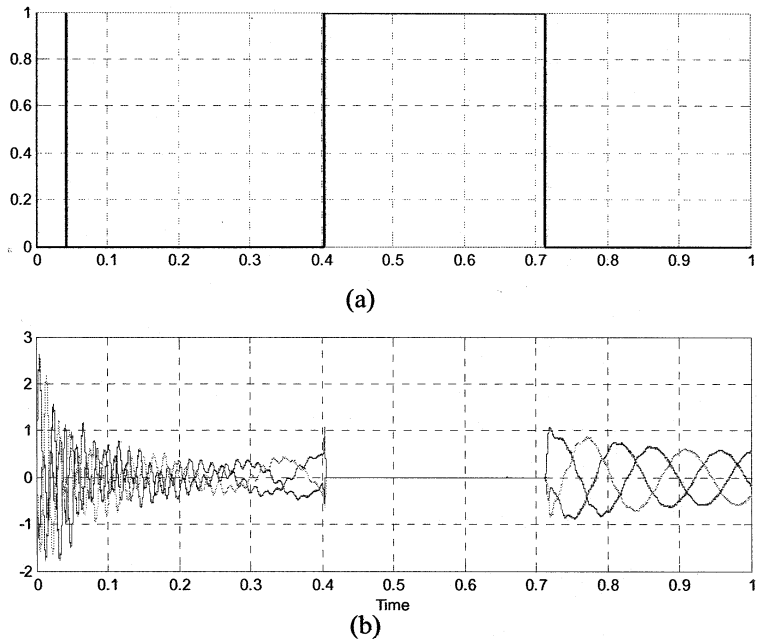

Figure 4-5 Rotor Current Response with Crowbar Activated, (a) Crowbar Enable, (b) Rotor Current

4.3.3 Fault Detection using Instantaneous Pseudo-Power Detection

The realization of independent active crowbar control is based on the fast detection. Three phase faults are much easier to detect through the voltage magnitude in the synchronous *dq* rotating frame because the fault is balanced – all three phases contain the same fault characteristic. Single phase and two phase faults are more difficult to detect as the voltage magnitude has a longer delay that may go undetected – the DFIG is capable of operating under these types of fault with no significant disturbance to the grid however it is not recommended.

Even though single phase and two phase faults are more difficult to detect, they do pose a serious problem to the rotor circuit. Excessive rotor currents under these fault conditions will induce damage to the machine side VSC. The underlying characteristic of these two fault conditions is the positive and negative sequence component in the stator voltage

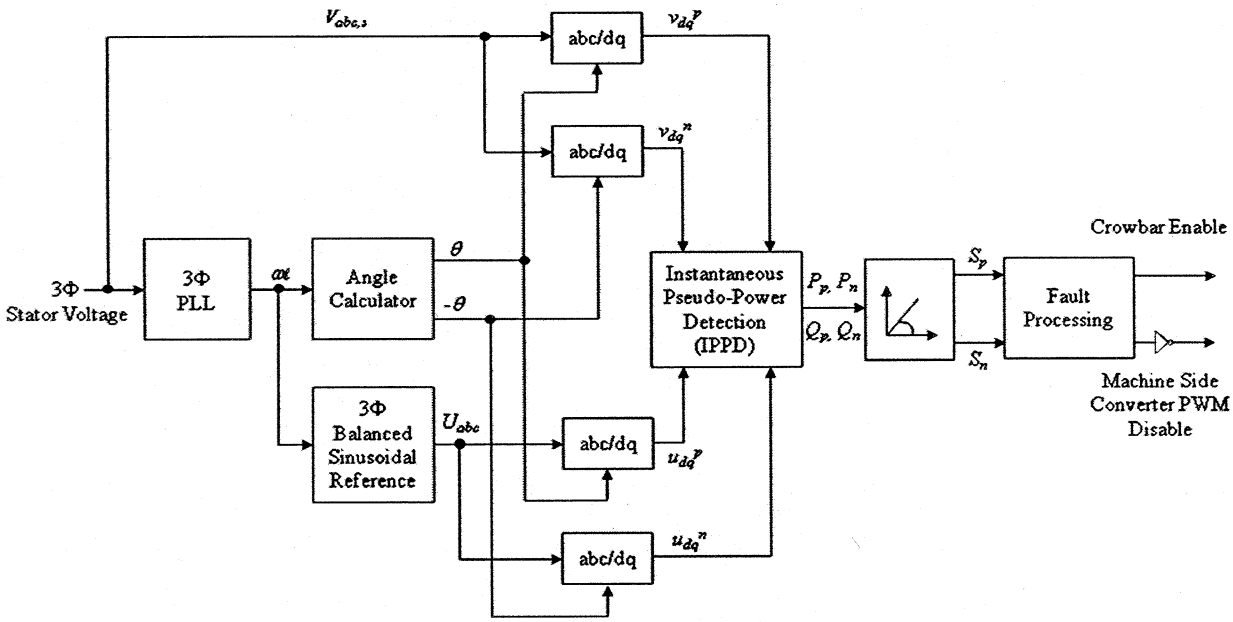

Figure 4-6 Instantaneous Pseudo-Power Detection Control Block

In the detection method, instantaneous pseudo-power detection (IPPD) is calculated from the sensed voltage. As shown in Figure 4-6, the three-phase voltages are sensed and the synchronous angle is detected through a PLL. A three-phase positive sequence balanced reference current is generated with the magnitude of one. Then the sensed voltages and reference currents are transferred to the two rotating frames, one is rotating synchronous with the grid and the other one is rotating at the same speed but reversely. The positive sequence power and negative sequence power are calculated using Eqn. (4.2). Assume that the system is in positive sequence, then no (or very small) negative sequence power would be generated. The positive and negative power are compared to a predefined reference value to determine the fault status, which can also determines the type of fault.

$$\begin{aligned} P_p &= u_d^p v_d^p + u_q^p v_q^p \\ P_n &= u_d^n v_d^n + u_q^n v_q^n \\ Q_p &= u_d^p v_q^p - u_q^p v_d^p \\ Q_n &= u_d^n v_q^n - u_q^n v_d^n \end{aligned} \tag{4.2}$$

The apparent power term is defined as the magnitude of the active and reactive negative and positive power vectors, Eqn. (4.3); under fault conditions where negative sequence voltage appears in the stator phase voltage. Using the apparent power terms reflects the dominant negative sequencing component of the voltage vectors.

$$S_p = \sqrt{P_p^2 + Q_p^2}$$
$$S_n = \sqrt{P_n^2 + Q_n^2} \tag{4.3}$$

The positive apparent power term, S_p can be used to determine if a three phase short to ground type fault has occurred. This is done, by comparing S_p to the reference value because in normal operation S_p is the magnitude of voltage vector in synchronous frame. Any voltage drop below 80% of the nominal grid voltage constitutes a low voltage condition, therefore the crowbar is activated immediately. As soon as the grid voltage is restored above 80%, the crowbar is deactivated and the machine side converter resumes normal operation.

The negative apparent power term, S_n determines a single phase short to ground or two phase short together or to ground type faults. Because S_n is calculated based on the negative reference angle, this term has a dominant negative sequence component. Eqn. (4.4) describes rule of fault detection,

$$S_n \begin{cases} 0, \textit{no fault occured} \\ \textit{non zero, fault occured} \end{cases} \tag{4.4}$$

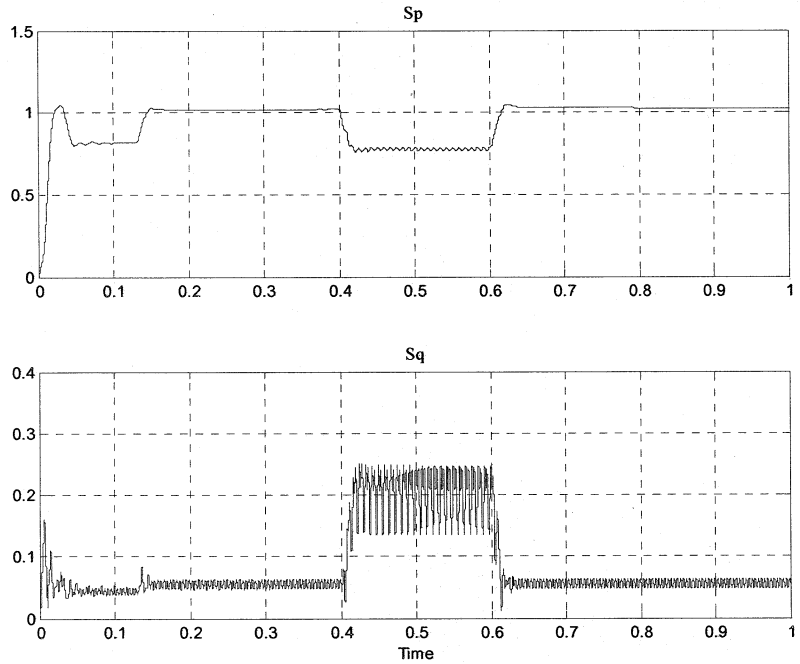

Figure 4-7 Positive and Negative Pseudo-Power during 1Φ Ground Fault

The IPPD response when a single phase short to ground has occurred is shown in Figure 4-7. Under normal steady operating conditions, S_n is approximately zero and S_p is 1.0 p.u indicating rated stator voltage. The introduction of the fault causes the S_p to decrease slightly to 0.8 p.u. however this term doesn't not trigger a single type fault condition because this value is within acceptable limits that define the turbine is operating normally. The fault is more evident in the S_n term, this value increases from zero and oscillates around 0.2 p.u. until the fault is removed. The oscillations are a result of the negative sequence component imposed on each of the phase voltages. Low pass and notch filters can reduce this ripple, however the addition of such filters without optimization can slow down the response of the protection functionality causing delays in the active crowbar response.

4.4 DFIG with Fault Detection System

The power circuit of the DFIG with the active crowbar protection is illustrated in Figure 4-8. In this section the behaviour of the DFIG will be analyzed with the IPPD method under different

fault conditions. It should be noted that the simulation data between time 0 and 0.4 seconds is irrelevant to the active crowbar performance. Focus will be put on the fault duration after 0.4s.

The machine side converter PWM gating signal is disabled by the IPPD block when the crowbar is activated. In conjunction with the IPPD control algorithm, the DC link voltage provides an additional protection method, which is usually used inside the control system. In the case of excessive rotor current being developed under fault conditions, over charging the DC link capacitor can cause damage and over stress to the component. Therefore a threshold value was defined with respect to the DC link nominal value, if the DC link voltage exceeds 120% of the nominal rating, the active crowbar will be activated in order to reduce the excessive voltage. However under fault conditions, the DC link voltage provides valuable information for system protection, therefore the redundancy built into the active crowbar control block is required.

4.4.1 Three Phase Shorted to Ground

Initially, the active crowbar protection block utilized S_p in diagnosing the occurrence of three phase shorts to ground occurring somewhere along the grid. Using this term was thought of as being the ideal scenario as the turbine's performance can be deduced directly from the apparent power characteristic; the inherent behaviour of the turbine under said fault condition is evident in both the DFIG control scheme and output variables.

The IPPD control block continuously monitored S_p and compared it to a predefine value corresponding to the LVRT characteristic, in this case, any value lower then 0.8 p.u. would signal a fault and activate the active crowbar. This method of control contributed to a large current transient shown in Figure 4-9, exceeding 2.0 p.u and lasting for 7.0 μs. The current spike is a direct result of the controller's response and the switching action of the active crowbar.

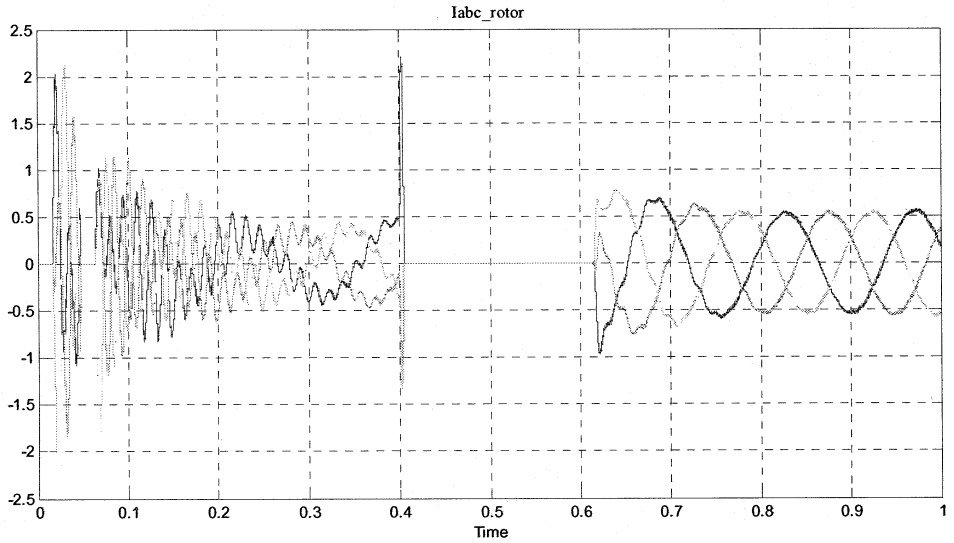

Figure 4-8 Rotor Current during 3Φ Fault using Sp Detection

Overcoming this problem was simply solved by comparing the magnitude of the v_{ds} and v_{qs} with respect to the limits set in the LVRT characteristic. This method offered an instantaneous response which can be seen in Figure 4-9 as the fault is injected into the grid, the rotor current does not exceed 1.0 p.u during crowbar activation. Manipulating the stator voltage within the control block still encompasses the principles outlined in the IPPD, however IPPD is tailored to annunciate negative sequencing and no such characteristic is inherent in three phase shorts to ground type faults.

The impedance of the active crowbar was set to 1.0 Ω limiting the current. The transient current spikes seen at 0.7 s is the instant when the machine side converter comes back online and the crowbar is removed form the system. The large transient current can be easily removed by limit the reference of current regulator and increase the current loop bandwidth.

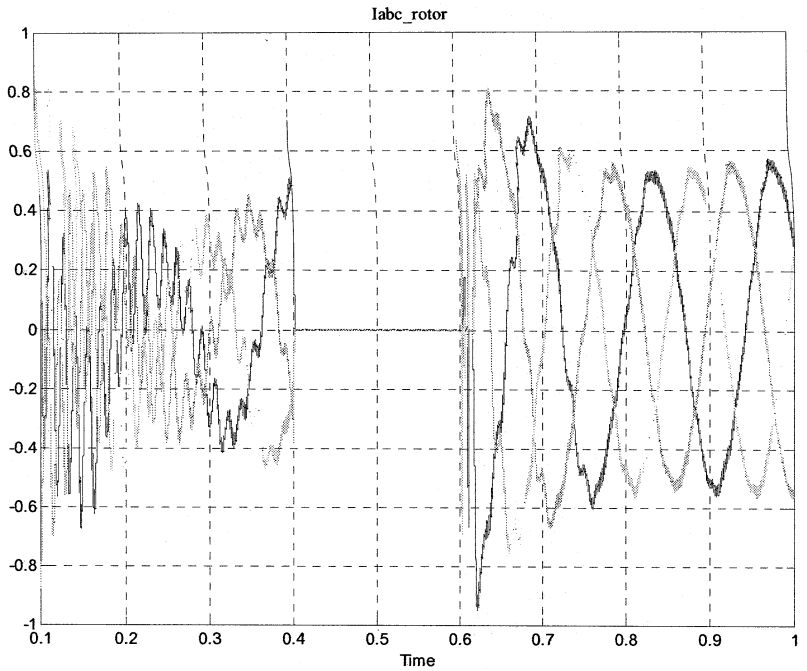

Figure 4-9 Rotor Current under Instantaneous Stator Voltage Control

The DFIG control regulates the DC link voltage to its nominal value while keeping the reactive power Q_s at zero. The DC link voltage increases slightly at the first rotor current peak. Even with the IGBTs in the machine side converter disabled by the IPPD, the energy continues to flow through the free-wheeling diodes leading to a very fast voltage increase lasting a very short duration [14]. Even though the DC link voltage remains relatively constant, the active power, P_s and stator voltage both drop to zero while the stator current increases in order to compensate for this loss. With the machine side converter disabled, no energy is transferred from the grid side converter, even though the grid side controller attempts at sustaining the voltage by means of adjusting the PWM gating pattern. Upon removal of the fault, the rotor current increases to 0.8 p.u. At this instant the machine side converter extracts energy from the DC link capacitor increasing P_s at 0.7 seconds.

The overall system performance of the DFIG with the active crowbar under this fault condition does not drastically impede the system behaviour as well, has no negative impact on the grid or connected loads, refer to Figure 4-10. Loads connected to generating systems that experience such faults have a tendency of drawing reactive power as a result of the impedance along the line

and the generation system under such conditions, however in the simulation, as P_s decreases to zero, Q_s remains unchanged – the controller does a good job of regulating the reactive power.

Similarly, the rotor speed remains relatively constant; due to the generator's large moment of inertia, observing any change in the rotor speed would be difficult under any fault condition lasting a few hundred milliseconds. Fault conditions longer then the LVRT characteristic would be required to trip off line preventing damage and equipment failure.

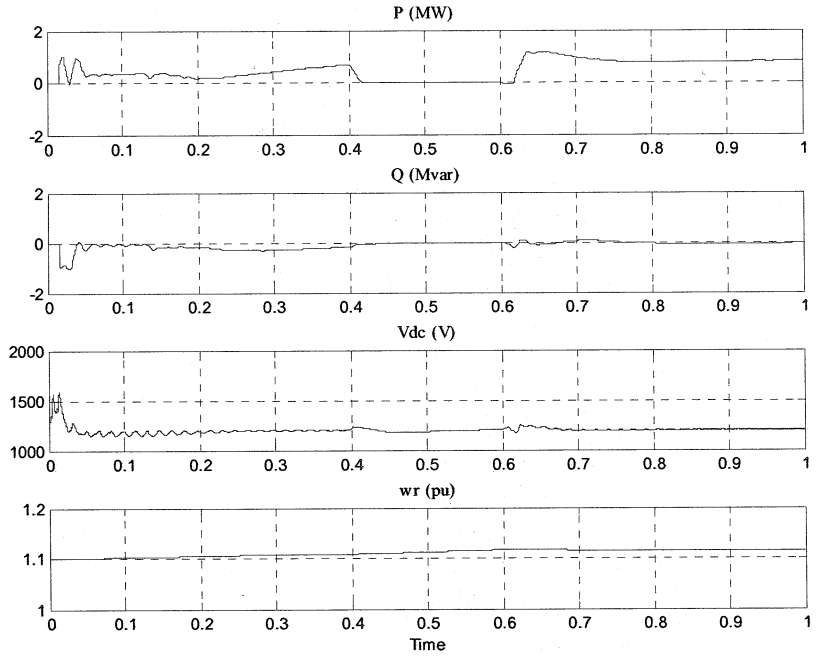

Figure 4-10 DFIG Characteristic with Active Crowbar under 3ϕ Short

4.4.2 Single Phase Shorted to Ground

Single phase fault conditions were determined by monitoring the amplitude of S_n with limits that define a single phase short fault condition. The challenge with this method was distinguishing between S_n and the ripple imposed on the signal. The current transient developed at the instant when the crowbar is activated is dependent on the controller's response, therefore it was observed, widening this limit impacted the transient peak by delaying the controller's response. Similarly, tightening this limit restricts the controller to detect a specific sequence which can be a combined with noise causing the response to be intermediate.

At the instant when the crowbar is activated, the rotor current transient increases beyond 1.0 p.u lasting only 5.0μs but is still within the acceptable device maximum rating. This scenario is not preferred as the objective is to reduce the affect of excessive rotor current on the power electronic equipment during fault conditions such that the device is not over stressing.

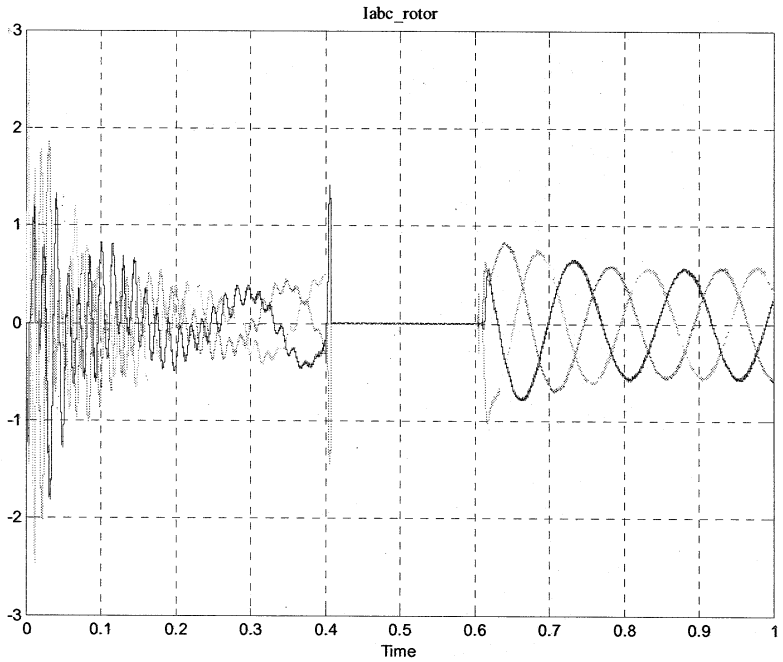

Figure 4-11 Rotor Current under Single Phase Fault with Active Crowbar

There is very little change in DFIG characteristic as seen in Figure 4-12, as the DC link voltage remains unaffected and the rotor speed slight increases still maintaining a speed above the synchronous speed.

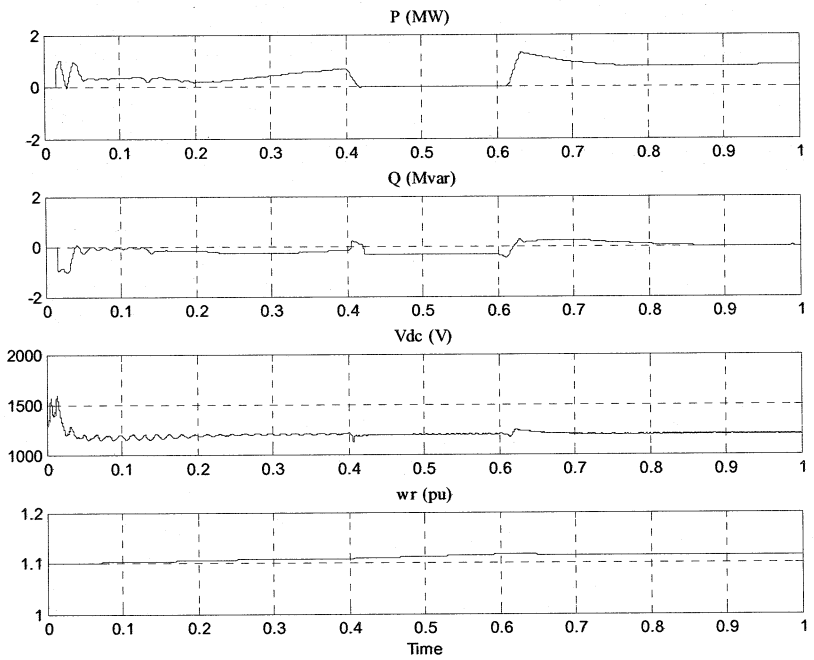

Figure 4-12 DFIG Characteristic with Active Crowbar under Single Phase Fault

4.4.3 Two Phase Shorted

The behaviour of the DFIG under a two phase fault condition is similar in nature when exposed to a single phase fault; the generator can still function even with the loss of a single phase. Two-phase short circuit has more severe impact to the machine side converter. From Figure 4-13, S_p decreases to 0.5 p.u. and S_n increases to 0.5 p.u. this means the generator is operating at 50% of its full capability. Even with the generator appearing to operate relatively normal, if not protected the rotor current exceeds the device ratings and can cause equipment failure.

In order to detect the fault, utilizing the fact the turbine is operating at half its capability, the fault detection processing block set the upper and lower limits of S_p to 10% of the nominal value. This method provided more flexibility with a faster response then implementing S_n in the detection.

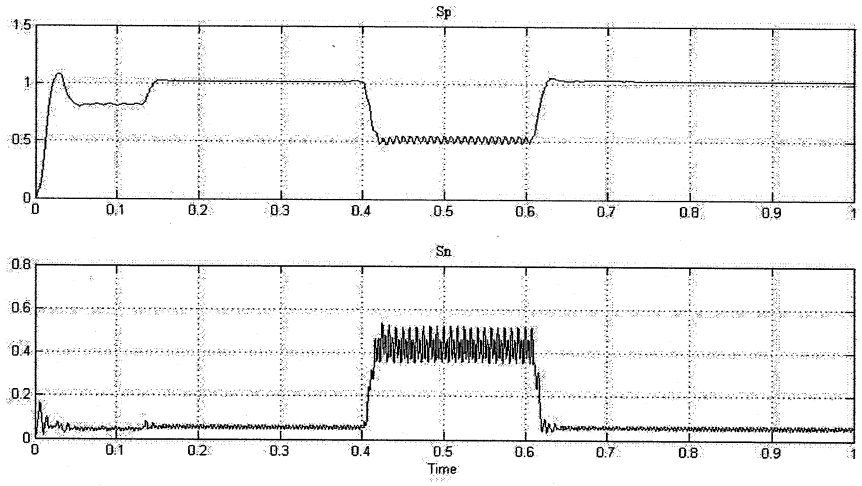

Figure 4-13 Apparent Power Terms under Two Phase Fault Condition

The negative sequencing component is dominate in S_n as its profile in Figure 4-13 satisfies Eqn. (4.3), however using this term in determining the fault did not provide instantaneous controller response. Due to the AC ripple imposed on S_n a delay of 10.0 μs was observed in the active crowbar enable signal which resulted in a current transient exceeding 2.0 p.u.

The response of the detection algorithm implemented to detect two phase faults is comparable to the method used in detecting three phase faults. In three phase fault conditions, the detection using IPPD is not fast enough. Then the stator voltages are directly transferred to the *dq* reference frame. The detection using the magnitude in *dq* reference frame is much faster then IPPD. This is evident in the rotor current profile seen in Figure 4-14. The rotor current quickly decreases to zero with no transient overshoot as the crowbar is activated. The possibility of damaging the power electronic equipment is negligible since the current overshoot is kept below 1.0 p.u. which is within acceptable device rating limits.

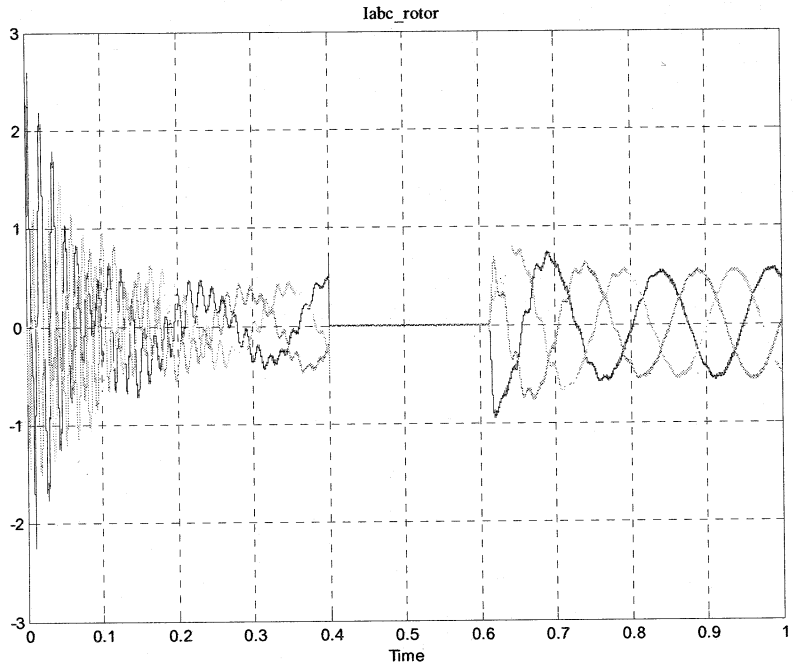

Figure 4-14 Rotor Current under Two Phase Fault Condition with Active Crowbar

4.5 Summary

In this chapter, several fault detection method was discussed. IPPD method combined with stator voltage detector was proposed for a standalone system with fast response. The proposed detection method only use generator stator voltage, which requires the voltage sensors, is less expensive than the method of modifying the control system or adding additional rotor side current sensors. The simulation results show that the converter transient current is successfully suppressed within 1.0 p.u. during fault, which is tolerable for most of the converter system. The DC current is suppressed within 120% when three-phase fault happens with proposed detection method and active crowbar.

CHAPTER 5 CONCLUSIONS

5.1 Conclusions

In the last twenty years, the wind energy, as one of the most promising renewable energy sources, has been seen fast growing world wide. The energy in wind is extracted by wind turbine and converted by generator into electrical energy, feeding the existing power system. Variable speed doubly-fed induction generator based wind energy conversion system has dominant the variable speed wind energy system in the last ten years. Many systems have been installed and the penetration rate of wind energy is increasing every year. Due to the nature uncertainty of wind energy resources, the high penetration rate causes some new instability problems for power system, which requires the WECS has the capability of fault ride through. For the existing system fault ride-through requirement forces the owners to consider the expensive system upgrade as well as the additional investment for protection during fault.

The research work based on DFIG wind energy system focus on the standalone solution for fault ride through. The control system and normal operation of DFIG based wind energy system was analyzed by simulation. Then the behaviour of converter, controller and generator was simulated under different fault conditions. The high transient rotor current and dc link voltage would be harmful for DFIG during fault. The problems of traditional solution of fault protection, such as tripping and re-connection were discussed in the project. Tripping WECS off-line causes the power system unstable due to the large wind farm reconnection and non-controllable power generation.

The DFIG based WECS can be upgraded inside the control system, where the rotor current is detected and active crowbar is employed to short the rotor circuit, in order to by-pass the excessive rotor energy to crowbar resistance. The machine side converter can be protected by disabling the gating signal when the crowbar is activated. The solution can be done by upgrading or in the newly designed system. In this project, a novel fault detection method is proposed based on IPPD. The method has fast response than other detection methods, which can be intensively used for a standalone crowbar, avoid the expensive system upgrade. The method can also be used to tell different faults, balanced or non-balanced effectively. The simulation results verified the proposed fault detection and protection for DFIG and rotor side converter.

5.2 Major Contribution

In this research project, the major contribution is the fast response fault detection method for a standalone crowbar. Crowbar is an effective solution for fault ride through in DFIG based wind energy system. But it usually needs the upgrade of control system or new design. The problems existed that the traditional fault detection methods through stator voltage have the one cycle time delay and sometimes are not suitable for unbalanced fault. The proposed IPPD based on instantaneous positive and negative sequence voltage magnitude has fast response. The simulation results verify that the proposed method is effective to protect the machine side converter from over current, which enable the WECS ride through the fault, no matter balanced three-phase fault or non-balanced faults.

5.3 Future Work

In this report, the fault detection method was proposed and simulated, future work can be done on the following aspect to make the system fully independent of the existing installed WECS.

1) The system need to be thoroughly verified through simulation and experiment. The simulation has been done on different fault conditions. But the relation between response time and converter tolerable over current has not been fully investigated.

2) The dc link is still detected in the system to be the redundancy as the fault detection. The detection of dc link is usually done in the controller for dc link voltage control. The dc link voltage detection may be removed if the fault detection is robust.

3) The control of active crowbar. The dissipation of rotor energy depends on the voltage dip and slip. The crowbar can be controlled through phase angle control to have better performance for the generator during fault.

REFERENCES

[1] http://en.wikipedia.org/wiki/Wind_energy#Turbine_placement

[2] Piwko, R.; Miller, N.; Sanchez-Gasca, J.; Xiaoming, Y.; Renchang, D.; Lyons, J.; Integrating Large Wind Farms into Weak Power Grids with Long Transmission Lines; Transmission and Distribution Conference and Exhibition: Asia and Pacific, 2005 IEEE/PES, 2005, pages 1 – 7

[3] http://www.ewea.org

[4] Muljadi, E.; Butterfield, C.P.; Pitch-controlled variable-speed wind turbine generation; IEEE Transaction on Industry Applications, Vol. 37, No. 1, 2001, pages 240-246

[5] Nunes, M.V.A.; Lopes, J.A.P.; Zurn, H.H.; Bezerra, U.H.; Almeida, R.G.; Influence of the variable-speed wind generators in transient stability margin of the conventional generators integrated in electrical grid; IEEE Transaction on Energy Conversion, , Vol. 19, No. 4, 2004, pages 692-701

[6] Morren, J.; de Haan, S.W.H.; Ridethrough of Wind turbine with DFIG during a voltage dip; IEEE Transaction on Energy Conversion, Vol. 20, No. 2, 2005.

[7] Gomez, S.A.; Amenedo, J.L.R.; Grid synchronization of doubly fed induction generators using direct torque control; IEEE Conference Record of IECON '02, Vol. 4, 2002, pages 3338- 3343

[8] Nordic Grid Code, 2007; published for Nordic Grid by the Transmission System Operators (TSOs) in Denmark, Finland, Norway and Sweden.

[9] Abbey, C.; Joos, G; Effect of Low Voltage Ride Through (LVRT) Characteristic on Voltage Stability; IEEE Conf. Rec. of PESC '05, Vol. 20, 2005 pages 1901 – 1907

[10] Bing, X.; Fox, B.; Flynn, D.; Study of fault ride-through for DFIG based wind turbines; IEEE International Conference on Electric Utility Deregulation, Restructuring and Power Technologies, Vol. 1, 2004; pages 411 – 416

[11] Yongsug, S.; Tijeras, V.; Lipo, T.A; A Nonlinear Control of the Instantaneous Power in dq Synchronous Frame for PWM AC/DC Converter under Generalized Unbalanced Operating Conditions; IEEE Conf. Rec. of IAS '02; Vol. 2; 2002; pages 1189 – 1196

[12] Niiranen, J.; Voltage dip ride through of a doubly-fed generator equipped with an active crowbar; Nordic Wind Power Conference, Chalmers University of Technology, 2004.

[13] Ekanayake, E.; Holdsworth, L; Jenkins, N.; Control of DFIG Wind Turbines; IEE Power Engineer Journal, Vol. 17, No. 1, 2003, pages 28 – 32.

[14] Erlich, I.; Wrede, H.;Feltes, C.; Dynamic Behavior of DFIG-Based Wind Turbines during Grid Faults; Proc. of 4th Power Conversion Conference, 2007, pages 1195 – 1200.

[15] Abo-Khalil, A.G.; Dong-Choon, Lee; Se-Hyun, L.; Grid Connection of a doubly fed induction generators in wind energy conversion systems; Power Electronics and Motion Control Conference, Vol. 3, 2006, pages 1-5

[16] Patel. R. Mukund, "Wind and Solar Power Systems", CRC Press, New York, 1999

[17] Datta, R.; Ranganathan, V.T.; Variable-speed wind power generation using doubly fed wound rotor induction machine-a comparison with alternative schemes; IEEE Transaction on Energy Conversion, Vol. 17, No. 3, 2002; pages 414 – 421

[18] Sun, Tao.; Chen, Z; Voltage Recovery of Grid-Connect Wind Turbines after a Short-Circuit Fault; Proc. of IECON '03; Vol. 3, pages 2723 – 2728.

[19] Jeong-Ik, J.; Young-Sin, K.; Dong-Choon, L.; Active and Reactive Power Control of DFIG for Wind Energy Conversion under Unbalanced Grid Voltage; CES/IEEE 5th International Power Electronics and Motion Control Conference '06, Vol. 3,pages 1-5

[20] Pena, R.; Clare, J.C; Asher, G.M.; Doubly fed induction generator using back-to-back PWM converters and its application to variable speed wind-energy generation; IEE Proceedings on Electrical Power Application, Vol. 143, No. 3, 1996.

[21] Rabelo, B.;, Hofmann, W.; Optimal Active and Reactive Power Control with the Doubly-Fed Induction Generator in the MW Class Wind-turbines, IEEE Conf. Rec. of PEDS '01, Vol. 1, pages 53 – 58.

[22] Yamamoto. M, Motoyoshi. O; Active and Reactive Power Control for Doubly-Fed Wound Rotor Induction Generator; IEEE Transaction on Power Electronics, Vol. 6, No 4, 1991.

[23] Hopfensperger, B.; Atkinson, D.J.; Lakin, R.A.;Stator flux-oriented control of a doubly-fed induction machine with and without position encoder; IEE Proceedings on Electric Power Applications, ,Vol. 147, No. 4, 2000 pages 241-250

[24] IEEE 519 Standard, recommended practices and requirements for harmonic control in electrical power system, IEEE Std 519-1992, April 1993.

[25] Erlich, I.; Winter, W.; Dittrich, A.; Advanced grid requirements for the integration of wind turbines into the German transmission system, IEEE PESC, 2006, pages 7

[26] Ivo,. F.;, Teodorescu,. R.;, Blaabjerg, R.;, Andersen, B.;, Birk, J.;, Miranda. J.; Grid Code Compliance of Grid-Side Converter in Wind Turbine Systems; IEEE Conf. Rec. of PESC '06, pages 1 - 7

[27] Kemsley, R.;Pannell, G.; Barbier, C.; Cost-Effective Improvements in DFIG Performance Under Fault Conditions for Offshore Applications; Econnect Ventures Ltd, 2004.

[28] Pettersson, A.; Analysis, Modelling and Control of Doubly-Fed Induction Generators for Wind Turbines; Ph.D thesis, Chalmers University of Technology; Goteborg, Sweden, 2005, pages 7-18, 41-47, 74-75, 110-113

[29] Seman, S.; Niiranen, J.; Kanerva, S.; Arkkio, A.; Analysis of a 1.7MVA Doubly Fed Wind-Power Induction Generator during Power Systems Disturbances; Proceedings of the Nordic Workshop on Power and Industrial Electronics (NORPIE 2004), 2004, Trondheim, Norway, pages 14 – 16.

[30] Investigation of Different Methods to Control a Small Variable-Speed Wind Turbine With PMSM Drives; Journal of Energy Resources Technology, Vol. 129, No. 3, 2007, pages 200-213

[31] Shin-Kuan, C.; Chang, G.W.; A New Instantaneous Power Theory-Based Three Phase Active Power Filter; IEEE Power Engineering Society Winter Meeting, Vol. 4, 2000, pages 2687 - 2692

[32] Tsourakis, G.; Vournas, C.D.; Simulation of Low Voltage Ride Through Capability of Wind Turbines with Doubly Fed Induction Generator, Proc. of European Wind Energy Conference '06.

[33] Nunes, M.V.A.; Lopes, J.A.P.; Zurn, H.H.; Bezerra, U.H.; Almeida, R.G; Influence of the Variable-Speed Wind Generators in Transient Stability Margin of the Conventional Generators Integrated in Electrical Grids, IEEE Transaction on Energy Conversion, Vol. 19, No. 4, 2004, pages 692 – 701

[34] Arkan, M.; Unsworth, P.J; Stator Fault Diagnosis In Induction Motors Using Power Decomposition; Industry Applications Conference, IEEE 34th IAS '99,Vol. 3, pages 1908 - 1912

[35] Panda, D.; Benedict, E.L.; Venkataramanan, G.; Lipo, T.A.; A novel control strategy for the rotor side control of a doubly-fed induction machine; IEEE 36th IAS '01; Vol. 3, 2001, pages1695 - 1702

[36] Fengquan, Z.; Joos, G.; Abbey, C.; Voltage stability in weak connection wind farms; IEEE PESC, Vol. 2, 2005, pages 1483- 1488

[37] Erlich, I.; Bachmann, U.; Grid code requirements concerning connection and operation of wind turbines in Germany; IEEE PESC '05, Vol. 2, 2005, pages 1253 - 1257

[38] Chen, Z.; Spooner, E; Grid power quality with variable speed wind turbines; IEEE Transaction on Energy Conversion, Vol. 16, No. 2, 2001, pages 148 - 154

[39] Sorensen, P.; Hansen, A.; Iov, F.; Blaabjerg, F.; Donovan, M.; Wind Farm Models and Control Strategies; Report for RISOE, August 2005, ISBN 87-550-3322-9 (Internet).

[40] Muller, S.; Deicke, M.; De Doncker, R.W.; Adjustable speed generators for wind turbines based on doubly-fed induction machines and 4-quadrant IGBT converters linked to the rotor; IEEE IAS '00, Vol. 4, pages 2249 – 2254

[41] Protsenko, K.; Flexible Power Flow Control for Brushless Doubly Fed Induction Generator; Thesis, Ryerson University, Toronto, Ontario, 2007, pages 41-43

APPENDIX A

General Mathematic Transformations

Clark Transform

$$\begin{bmatrix} x_d \\ x_q \end{bmatrix} = \frac{2}{3}\begin{bmatrix} \cos\theta & \cos\left(\theta - 2\pi/3\right) & \cos\left(\theta - 4\pi/3\right) \\ -\sin\theta & -\sin\left(\theta - 2\pi/3\right) & -\sin\left(\theta - 4\pi/3\right) \end{bmatrix} \cdot \begin{bmatrix} x_a \\ x_b \\ x_c \end{bmatrix}$$

$$\begin{bmatrix} x_a \\ x_b \\ x_c \end{bmatrix} = \begin{bmatrix} \cos\theta & -\sin\theta \\ \cos\left(\theta - 2\pi/3\right) & -\sin\left(\theta - 2\pi/3\right) \\ \cos\left(\theta - 4\pi/3\right) & -\sin\left(\theta - 4\pi/3\right) \end{bmatrix} \cdot \begin{bmatrix} x_d \\ x_q \end{bmatrix}$$

APPENDIX B

Matlab/Simulink .M File

```
% Copyright 2005 TransEnergie Technologies Inc., under sublicense
%  from Hydro-Quebec, and The MathWorks, Inc.


NumberOfUnits=1;

% Asynchronous machine data
Pnom=1.5e6/0.9*NumberOfUnits; % Nominal power (VA)
Vnom=575;   % Line-Line voltage (Vrms)
Fnom=60;    %Hz
Rs=0.00706; %pu
Lls=0.171;  %pu
Rr=0.005;   %pu
Llr=0.156;  %pu
Lm=2.9;     %pu
H=5.04;     %Inertia constant (s)
F=0.01;     %Friction factor (pu)
p=3;        %Number of pairs of poles

%PWM data
PWM_freq=27*Fnom;                       %Not used with average model

%DC link
Vdc_nom=1200;                           %Volts
C_DClink=10000e-6*NumberOfUnits;        %Farads

%Choke data
R_RL=0.30/100;      %pu
L_RL=0.30;          %pu

%Turbine data
Pmec=1.5e6*NumberOfUnits;       % Nominal power (W)
power_C=0.73;                   %pu
speed_C=1.2;                    %pu
```

APPENDIX C

Simulink Model

Top Level Block Diagram:

Original file located: SimPowerSystems Demo → power_wind_dfig_det

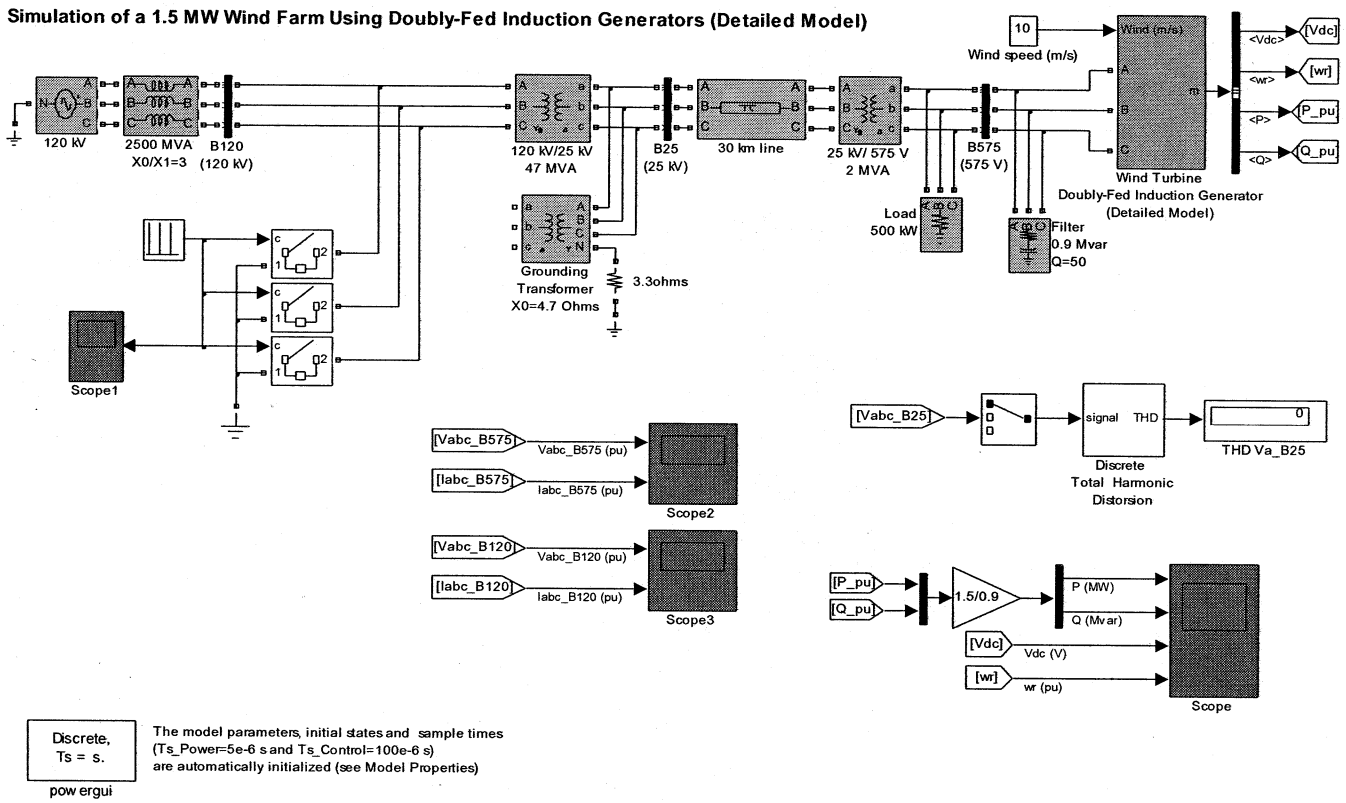

Block Name	Parameter	Value
120 kV	Amplitude [V_{RMS} phase-phase]	120,000V
	Phase [degree]	0°
	Frequency [Hz]	60

APPENDIX B

Matlab/Simulink .M File

```
% Copyright 2005 TransEnergie Technologies Inc., under sublicense
%  from Hydro-Quebec, and The MathWorks, Inc.


NumberOfUnits=1;

% Asynchronous machine data
Pnom=1.5e6/0.9*NumberOfUnits; % Nominal power (VA)
Vnom=575;    % Line-Line voltage (Vrms)
Fnom=60;     %Hz
Rs=0.00706;  %pu
Lls=0.171;   %pu
Rr=0.005;    %pu
Llr=0.156;   %pu
Lm=2.9;      %pu
H=5.04;      %Inertia constant (s)
F=0.01;      %Friction factor (pu)
p=3;         %Number of pairs of poles

%PWM data
PWM_freq=27*Fnom;                    %Not used with average model

%DC link
Vdc_nom=1200;                        %Volts
C_DClink=10000e-6*NumberOfUnits;     %Farads

%Choke data
R_RL=0.30/100;     %pu
L_RL=0.30;         %pu

%Turbine data
Pmec=1.5e6*NumberOfUnits;    % Nominal power (W)
power_C=0.73;                %pu
speed_C=1.2;                 %pu
```

Block Name	Parameter	Value
30 km Line	Frequency [Hz]	60
	Positive-sequence resistance [Ω/km]	0.1153
	Zero-sequence resistance [Ω/km]	0.413
	Positive-sequence inductance [H/km]	1.05m
	Zero-sequence inductance [H/km]	3.32m
	Positive-sequence capacitance[F/km]	11.33p
	Zero-sequence capacitance [F/km]	5.01p
	Line section length [km]	30

Block Name	Parameter	Value
25 kV/575 V 2 MVA	Nominal Power [VA]	2,000,000
	Frequency [Hz]	60
	Winding 1 Connection [ABC]	Y_g
	Winding 1 Voltage [V_{RMS} Ph-Ph]	25,000
	Winding 1 Resistance [p.u.]	0.025/30
	Winding 1 Inductance [p.u.]	0.025
	Winding 2 Connection [abc]	Delta (D1)
	Winding 2 Voltage [V_{RMS} Ph-Ph]	575
	Winding 2 Resistance [p.u.]	0.025/30
	Winding 2 Inducatance [p.u.]	0.025
	Magnetization Resistance [p.u.]	500
	Magnetization Reactance [p.u.]	infinity

Block Name	Parameter	Value
Load 500 kW	Configuration	Y (grounded)
	Nominal voltage [V_{RMS} Ph-Ph]	575
	Active Power P [W]	500,000
	Inductive reactive power [positive var]	0
	Capacitive reactive power [negative var]	0

Block Name	Parameter	Value
Filter 0.9 Mvar Q = 50	Configuration	Y (grounded)
	Nominal voltage [V_{RMS} Ph-Ph]	575
	Active Power P [W]	150,000/50
	Inductive reactive power [positive var]	0
	Capacitive reactive power [negative var]	150,000/50

Wind Turbine Doubly-Fed Induction Generator (Detailed Model)

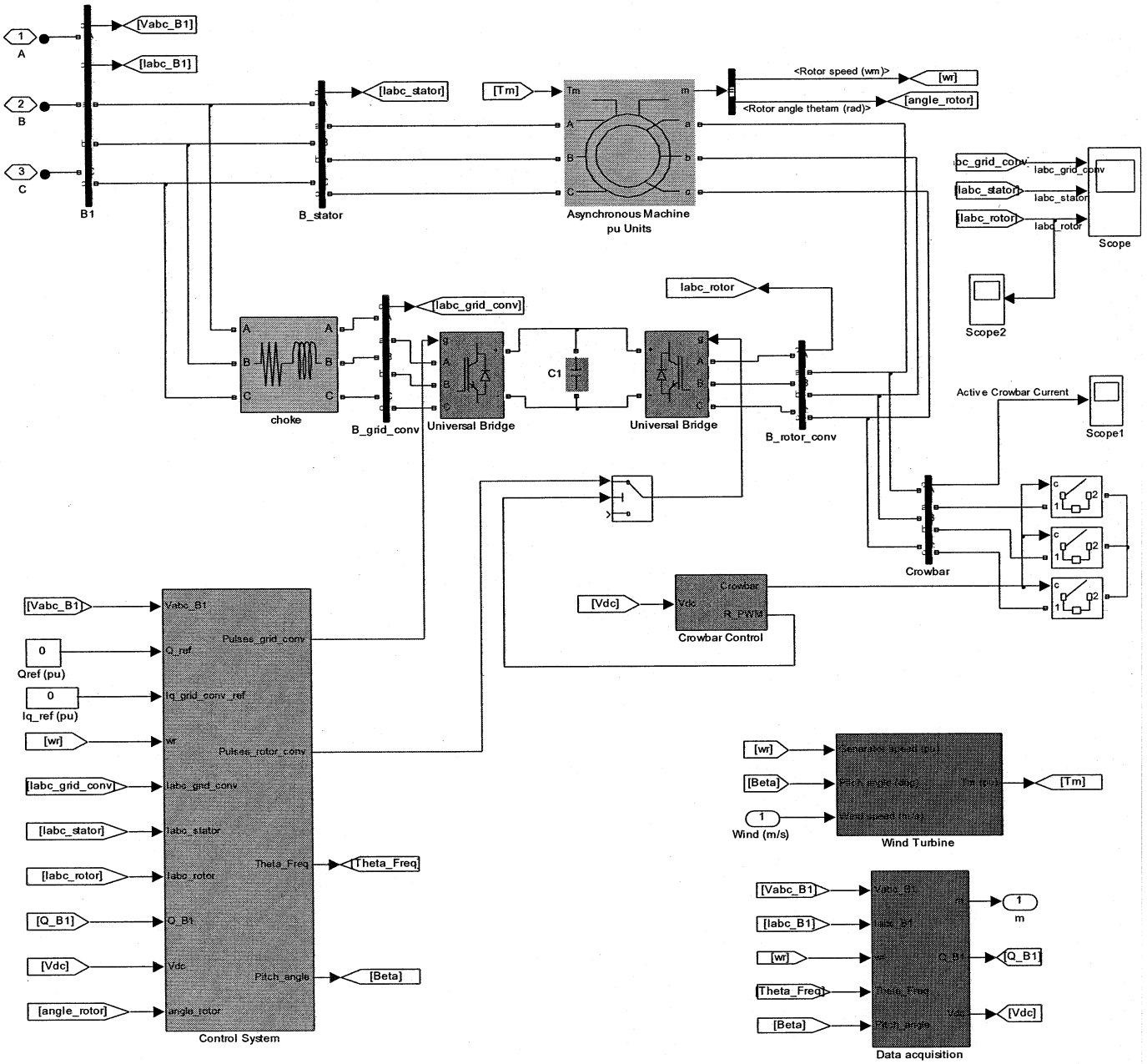

Block Name	Parameter	Value
Asynchronous Machine	Mechanical input	Torque, T_m
	Rotor Type	Wound
	Reference Frame	Stationary
	Nominal Power [VA]	1.5M/0.9
	Nominal Voltage [line-line]	575
	Nominal Frequency [Hz]	60
	Stator Resistance [p.u.]	0.00706
	Stator Inductance [p.u.]	0.171
	Rotor Resistance [p.u.]	0.005
	Rotor Inductance [p.u.]	0.156
	Mutual Inductance [p.u.]	2.9
	Inertia Constant [s]	5.04
	Friction Factor [p.u.]	0.01
	Pole pairs	3

Block Name	Parameter	Value
Control System	Converter maximum power [p.u.]	0.5
	Nominal DC bus voltage [V]	1200
	DC bus capacitor [F]	
	Tracking characteristic speed_A [p.u.]	0.7
	Tracking characteristic speed_B [p.u.]	0.71
	Tracking characteristic speed_C [p.u.]	1.2
	Tracking characteristic speed_D [p.u.]	1.21
	Power at point C [p.u./P_{Mech}]	0.73
	Pitch angle controller gain [K_p]	500
	Maximum pitch angle [degree]	45
	Maximum rate of change of pitch angle [degree/second]	2
	Reactive power regulator gains [K_p K_i]	[0.05 5]
	DC bus voltage regulator gains [K_p K_i]	[0.002 0.05]
	Grid-side converter current regulator gains [K_p K_i]	[2.5 500]
	Rotor-side converter current regulator gains [K_p K_i]	[0.3 8]
	Maximum rate of change of reference reactive power [p.u./second]	100
	Maximum rate of change of reference torque [p.u./s]	1.0
	Maximum rate of change of converter reference currents [p.u./second]	200

Block Name	Parameter	Value
Universal Bride	Number of bridge arms	3
	Snubber resistance [Ω]	1.0×10^{5}
	Snubber Capacitance [F]	Infinity
	Power Electronic Device	IGBT/Diodes
	Turn-on resistance [Ω]	1.0×10^{-4}

** Consider power electronic devices to be ideal

Block Name	Parameter	Value
Wind Turbine	Nominal mechanical output power [W]	1.5M/0.9
	Base power of the electrical generator [VA]	1.5 M
	Base Wind Speed [m/s]	11.0
	Maximum power at base wind speed [p.u. of nominal mechanical power]	0.73
	Base rotational speed [p.u. of base generator speed]	1.2